Chapter IV
Unsymmetrical nematogenic mesogens

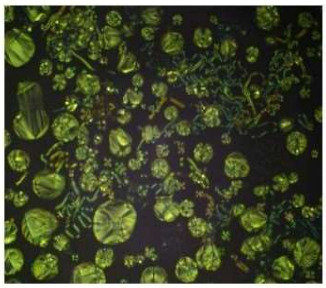

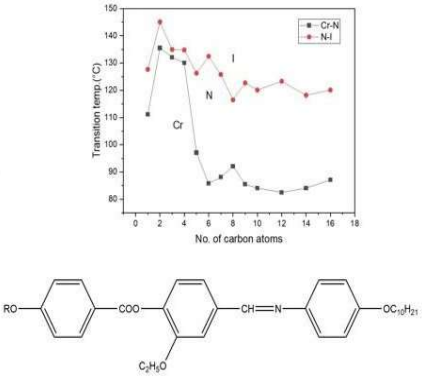

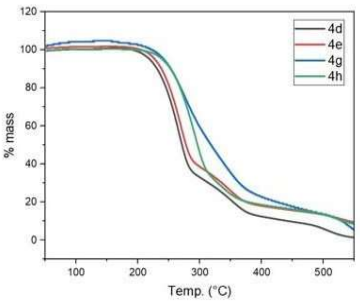

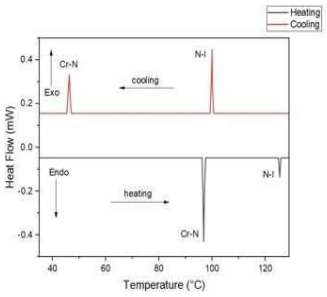

Synthesis, characterization, and study of unsymmetrical homologous series of nematogenic liquid crystal compounds possessing azomethine linkage

4.1. Introduction

The liquid crystalline state is a special state of matter that has gained significant importance and attention in both the basic sciences and technological applications. These advanced applications include digital displays, sensors, liquid crystal displays (LCDs), high-performance polymers, drug-delivery systems, digital displays, and hybrid composites. Calamitic mesogens, which are rod-shaped liquid crystalline materials with a rigid core, two or more aromatic rings connected by connecting groups, and flexible terminal chains, have garnered a lot of attention recently because of their capacity to exhibit a variety of crucial liquid crystal phases. They exhibit some possible applications by varying their physical properties, such as rotational viscosity, birefringence (Δn), dielectric anisotropy (Δε), and mesophase range for liquid crystal compounds, using a variety of rod-like molecular architectures. Liquid crystalline materials have the unique ability to provide molecules with greater flexibility and an orderly pattern [1]. Liquid crystals combine the visual qualities of solids with fluid-like arrangement. Although it is not as organized as the solid state, the liquid crystalline state has a more ordered molecular arrangement than the liquid state [2]. These days, liquid crystalline materials are used in thermosensors, chemical sensors, solar cells, bio-imaging, and optical storage systems [3–8]. The structure of a thermotropic LC molecule consists of a part that typically has a linker rod applied to join aromatic rings with the aid of various linking units and an end tail made up of straight alkyl or alkyloxy chains with a polar substituent as the terminal unit to provide flexibility and stability to the molecular alignment. The amount of carbon atoms in the alkyl chain determines how flexible the LC molecule is, and both nematic and smectic mesophases can form depending on the types of substituents and their combinations [9, 10]. Greater mesophase stability and enhanced dipole-dipole interactions with polarity and polarizability towards the molecular system are provided by the presence of a bigger lateral group on linear-shaped molecules [11–14]. Conversely, the lateral substituent groups effectively widen the molecular core and further increase the intermolecular separation because of the steric effect. This reduces the lateral associations of rod-shaped molecules, which in turn reduces the mesophase stability [15].

The shape of the great majority of liquid crystalline substances is either disc or rod-shaped. They typically display a columnar or lamellar mesophase. Many attempts have been undertaken to synthesize this kind of material since the unique property of achiral bent-core molecules of the production of a polar order mesophase was discovered [16-19]. Lateral groups have an impact on the molecular alignment and packing in liquid crystal materials. These groups can either help or impede the development of organized structures inside the material, depending on their size, shape, and chemical makeup. The expression of liquid crystalline features like anisotropic flow and birefringence depends on precise alignment. The phase behavior of liquid crystalline materials can be affected by lateral groups. When it comes to the transition between the nematic and smectic phases, for example, various lateral groups can result in different phase transition temperatures. Furthermore, the stability and range of existence of different phases might be impacted by lateral groups. Lateral groups can influence the thermal stability of liquid crystalline materials. Due to more intermolecular interactions or molecular motion, certain lateral groups may increase the material's thermal stability while others may lower it.

Research has demonstrated that the mesomorphic and physical properties of liquid crystals are significantly impacted by lateral substitution, with the degree of effect varying according to the type, quantity, and locations of lateral substituents inside the liquid crystalline molecular cores [20]. Since molecular packing affects mesophase stability [21], a deeper comprehension of liquid crystal features may result from examining intermolecular interactions, association events, and dipole-dipole correlations that impact molecular packing. One may assume that anything protruding from the side of a molecule with liquid crystal qualities would disturb the molecular packing, decreasing the stability of the liquid crystal phase [22]. Although lateral substitution is almost always the cause of this kind of disruption, the circumstances are quite crucial, and in many instances, the mesomorphic and physical qualities for applications benefit from this disruption to the molecular packing. The lateral substituent placements are significant because they have varying effects on the conjugation with the ring to which they are connected. However, there is also a noticeable impact on the substituent's size [23-26].

Intermolecular forces, due to intermolecular dispersion forces and dipole-dipole interactions, proved [27] to be a factor predominating in determining the mesophase stability of a liquid crystalline compound. On the other hand, linking groups containing multiple bonds, such as -N=N-, that maintain the linearity and rigidity within the molecule are also satisfactory. Furthermore, conjugative interaction affected by the ester -COO- group linking two aromatic rings also leads to some double bond character. Consequently, both the azo and ester groups

are considered good connecting groups to design new molecules with varying mesomorphism [28–42]. A lateral group linked to the nematic core generally has a major influence on the mesomorphic behaviour of a liquid crystalline molecule. The lateral substituent has a steric impact that widens the molecular core and increases intermolecular separation. This decreases the lateral affiliations of rod-shaped molecules, which in turn decreases the mesophase stability of the molecule [43–53]. It has been discovered that a lateral methyl substitution significantly lowers both the nematic stability and melting temperatures. However, within a homologous sequence, lengthening the terminal alkyl chain adopts the conformation along the mesogenic core; this results in a slight depression in nematic stability but does not further lower melting points [54]. Goodbye *et al*. [55,56] have demonstrated that free volume, which is influenced by molecular shape and its deformation, is another element that affects the kind and stability of the mesophase.

The nature of terminal chains, such as alkyl, alkyloxy, perfluorinated chain, ester or acyl group, or introduction of heteroatom into terminal chains, was found to have a major influence on the mesomorphic features of thermotropic calamitic LC [57-60]. Attractive mesomorphic features were seen in a range of materials synthesized based on five and six-membered heterocyclic rings containing one, two, or three nitrogen atoms. The position of nitrogen atoms and the availability of their lone pair of electrons are responsible for the heightened attractive forces and layer formation capabilities resulting from the molecular stacking and packing of these liquid crystals. Because lone-pair electrons on heteroatoms of rings exist, the addition of a heteroatom or heterocyclic unit often stimulates negative dielectric anisotropic properties. These effects include polarizability, enhanced lateral and/or longitudinal dipole moment, increased intermolecular interaction, an impact on mesophase stability, phase transition temperatures, and the introduction of transverse dipole moment [61]. Interesting mesomorphic features were demonstrated by mesomorphic compounds with five-membered heterocyclic units, such as thiophene, 1,2,4-oxadiazole, isoxazole, and 1,3,4-thiadiazole [62, 63]. Lately, several pyridine-based structurally varied liquid crystals have been formed and their mesomorphic characteristics were examined.

Additionally, several liquid crystalline compounds were synthesized and their liquid crystal behavior was examined. These compounds included imines, ester, ethers, and azo units to connect different aromatic rings. Researchers have been paying a lot of attention since the discovery of 4-methoxybenzylidene-4C-butylaniline at room temperature nematogen [64], as the insertion of Schiff base unit (-CH=N-) promotes the stability of mesophase by retaining the

stiffness and linearity. Lately, some low molar mass thermotropic mesogens based on Schiff base have been formed, examined, and characterized. The mesomorphic behaviour of liquid crystal compounds with a rod-like structure is mostly dependent on the molecular conformation of the molecule. Mesogen's mesomorphic characteristics are greatly altered by even small structural modifications. Furthermore, the mesogenic chemicals terminal groups/chains and central linking unit have a major role in the creation of the mesophase, the kind of phase, and its thermal stability [65, 66]. Therefore, the connecting unit, terminal groups, and flexible hydrocarbon chains are essential in the construction of novel mesogenic chemicals.

The temperature fluctuations and temperature range of thermotropic mesomorphic substances rely on the rigidity and flexibility of their molecules, which are derived from their different molecular structures [67]. The presence of mesophases at lower temperatures is critical for prospective commercial applications. The phase transition temperatures are lowered in large part by lateral substituents.

The mesomorphism of a substance and its molecular structure are closely related. It is difficult to characterize a molecule's characteristic structure that will reveal its mesomorphic state, though. The only substances that are known to display a liquid crystalline form are organic ones. Both aliphatic and aromatic substances exhibit mesomorphism. Whereas the simplest aromatic compound and the simplest aliphatic molecule that exhibits liquid crystallinity is 2,4-nonadienoic acid. It is possible to explain the presence of mesomorphic states by taking into account the molecular makeup of substances that exhibit mesomorphic behavior. It is noted that forces which emerge from a rod-shaped molecule's anisotropic shape can cause the liquid crystal phases to form. The need that a nematogen's molecule to have a very stiff core structure, typically with terminal substituents attached. Chemists have been attempting to comprehend the variables that link the features of liquid crystals to molecular structure. This has been somewhat successful for some properties, such as liquid crystal transition temperatures, but more work remains for other properties, such as elastic constants and molecular dynamics.

4.1.1 Effect of the Core:

The rigid unit made up of ring units connected linearly is known as the core. It is frequently used to refer to any connecting units attached to the structure. An optical anisotropy that is quite high (birefringence) and a positive dielectric anisotropy are conferred by the aromatic core in conjugation with a terminal cyano group. More importantly, they are stable both chemically and photochemically, and they have a relatively low viscosity. These materials are still effectively utilized in low-tech twisted nematic display displays, such as those seen in

watches and calculators. The anti-parallel correlations present in this core contribute to its high nematic phase stability (T_{N-I}) values, which in turn increase the real molecular length. The feasible materials used in devices were the alkylcyanobiphenyls (Compound **(I)).** The compounds have high T_{N-I} values and low melting points. Compound **(II)** exhibits a significant rise in T_{N-I} due to the addition of a third aromatic ring, which lengthens the linear core, increases the length-to-breadth ratio, and increases the polarizability anisotropy. This chemical extends T_{N-I} in commercial nematic biphenyl combinations.

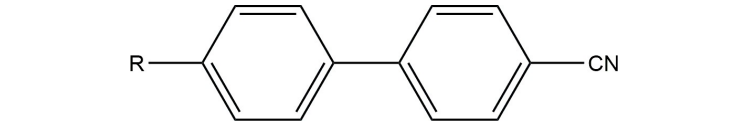

(I)

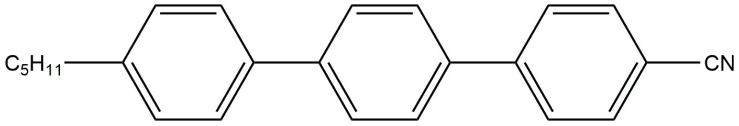

(II)

Figure 4.1: Liquid crystal compounds containing core groups

4.1.2 Effect of Linking Groups:

Linking groups are consistent with the rest of the structure and preserve the linearity of the core. Compounds (**IV)** and (**V**) are related materials that often display the nematic phase, while the parent compounds (like compound **(III)**) typically exhibit smectic phases.

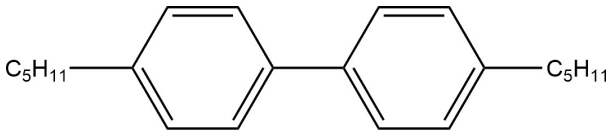

Cr 26.0 Sm 47.6 Sm 52.2 Iso

(III)

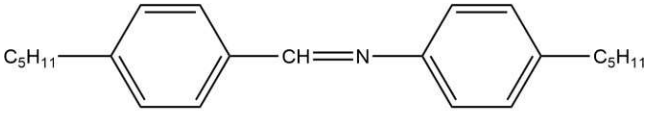

Cr 34.5 (SmB 32.0) N 43.7 Iso

(IV)

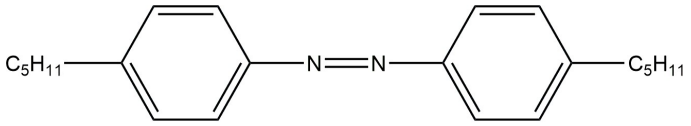

Cr 49.5 (N 38.0) Iso

(V)

Figure 4.2: Liquid crystal compounds containing linking groups

The functional group ester is the most widely utilized connecting unit due to its low melting point capability, ease of synthesis, and relative stability. The ester linkage is not a fully conjugative unit, but it is a planar connecting group with some polarizability because of the π-electrons connected to the carbonyl group. Because of this, the ester is a flexible linking unit that may be applied in a variety of molecular contexts.

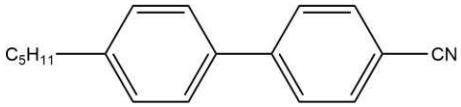

Cr 24.0 N 35.0 Iso

(VI)

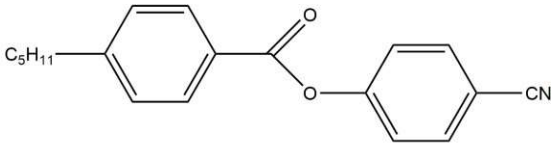

Cr 64.5 (N 55.5) Iso

(VII)

Figure 4.3: Liquid crystal compounds containing ester linking group

Compound (**VII**) ester unit has improved the T_{N-I} compared to the directly linked compound (**VI**). Still, the melting point has increased further, leaving just a monotropic nematogen.

In Compound (**VIII**), ethylene linkage increases the molecule length while preserving linearity; as a result, the T_{N-I} value is quite high. In Compound (**IX**) acetylene linkage prolongs the molecular length while preserving the core's stiffness, linearity, and polarizability. Despite being substantially greater than the parent cyanobiphenyl (**VI**), the T_{N-I} value of compound (**IX**) is still lower than that of compound (**VIII**) due to the lower polarizability and less efficient conjugation of the linkage.

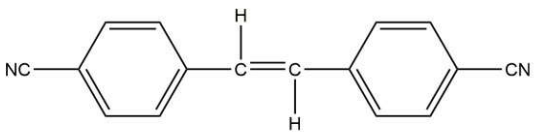

Cr 55.1 N 101.0 Iso

(VIII)

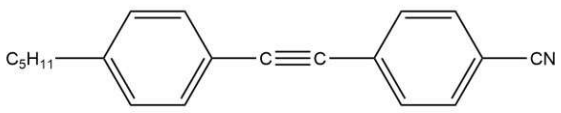

Cr 79.5 (N 70.5) Iso

(IX)

Figure 4.4: Liquid crystal compounds containing linking groups

4.1.3 Effect of Terminal Substituents:

At least one terminal alkyl/alkoxy chain can be found in most liquid crystal molecules. These chains are in charge of maintaining the molecular orientations required for the formation of the mesogens. To stabilize molecule orientation, polar groups allow for large and significant intermolecular forces of attraction. According to Maier and Saupe's hypotheses, the compound's nematic-isotropic transition temperature is correlated with its molecular polarizability, which is inevitably tied to the terminal group and how it affects molecule conjugation.

Because longer chains are more flexible, they have lower melting points. However, when chains are exceedingly long, the weak chemical forces of attraction lead the melting points to rise, necessitating a compromise in length to achieve low melting points. Although it does start to rise with very long compound terminal chains, the T_{N-I} value falls with increasing chain length. On the other hand, odd-member chains produce greater T_{N-I} values than even-member chains in the T_{N-I} value trend. This can be explained by the additional carbon that gives the chain its extra strength by forming a derivation from the straight chain structure of the chain's more advantageous all-trans conformation, as compounds **(X)** and **(XI)** demonstrate. The smectic tendency grows with terminal chain length and eventually drives out the nematic phase. Hence the longer chains entangle and get attracted to one another, facilitating the lamellar packing necessary for the formation of the smectic phase. Materials behave differently in liquid crystal phases when their alkyl chains are branched. Of particular importance is the ability to introduce chirality into a molecule by chain branching. A terminal chain's branching disturbs the molecular packing, which frequently lowers melting temperatures and inevitably lowers the stability of the liquid crystal phase. A low melting point is caused by much-increased disruption when the branch is near the core.

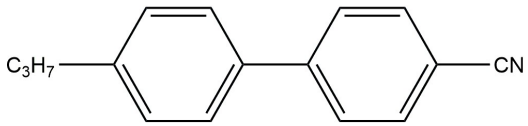

Cr 66.0 (N 25.5) Iso

(X)

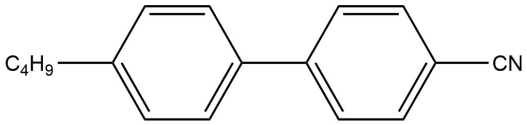

Cr 48.0 (N 16.5) Iso

(XI)

Figure 4.5: Liquid crystal compounds containing linking groups

4.1.4 Effect of Lateral Substituents:

Attached to the molecule's linear axis, a lateral substituent is typically found on the side of an aromatic core. However alicyclic moieties have also been shown to contain lateral substituents. On a cyclohexane ring, lateral cyano groups and fluoro substituents have been synthesized in a variety of materials. Numerous distinct liquid crystal systems have been combined with a broad variety of lateral substituents, such as F, Cl, CN, NO_2, CH_3, and CF_3. Although lateral substitution is significant in both smectic and nematic systems, it almost invariably decreases smectic phase stability more than nematic phase stability due to the unique disruption to the lamellar packing required for smectic phases. On the other hand, the use of a polar lateral substituent can somewhat offset the depression of smectic phase stability caused by a lateral substituent. Increasing size disturbs lamellar packing, but increasing polarity strengthens it.

The fluoro substituent is the most often utilized lateral substituent. The size of the fluoro substituent is quite small. A steric effect is produced by a lateral fluoro substituent. Furthermore, the fluoro substituent exhibits a significant degree of polarity.

Compound **(XII)** lateral fluoro substituent lowers the melting point relative to compound (**VII**) and results in a comparable decrease in T_{N-I}. Compound **(XIII)**, a second fluoro substituent, is added, and this lowers the T_{N-I} value even further without barely changing the melting point.

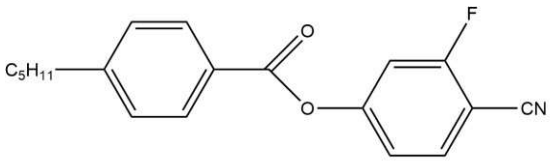

Cr 30.5 (N 24.5) Iso

(XII)

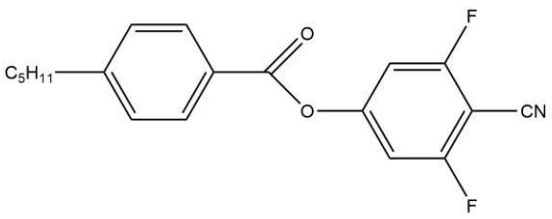

Cr 29.5 (N -8.0) Iso

(XIII)

Figure 4.6: Liquid crystal compounds containing lateral substituents

Materials exhibiting the SmC phase and suitable for use as ferroelectric host materials have been produced through the widespread usage of lateral fluoro substitution. Molecule tilting may result from a lateral dipole produced by a lateral fluoro substituent. Fluoro substitutes work best with compounds with a strong smectic property, which is not always tilted. The smectic character is greatly reduced by the fluoro substituent, although the smectic character that remains is frequently skewed. Furthermore, extremely smectic materials are frequently transformed into pure nematogens with low melting temperatures by adding a lateral fluoro substituent.

In the present chapter, we have prepared unsymmetrical homologous series of nematogenic liquid crystal compounds possessing imine linkage incorporated in a molecule with an alkoxy group (n = 1-10, 12, 14, 16) attached at one of the terminal end and 4-n-decyloxy aniline at another terminal end of the molecule and studied the liquid crystalline behavior of all the compounds. Homologous series consisting of thirteen derivatives were synthesized and their physical and chemical properties were studied.

The general chemical structure is shown below:

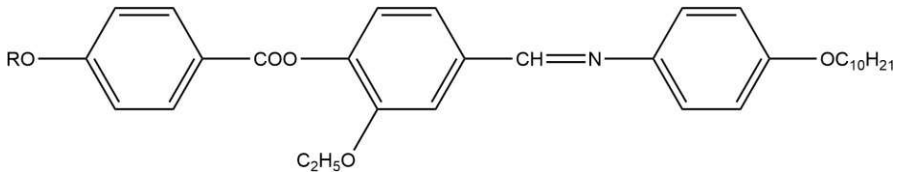

Where R = -C_nH_{2n+1}, where n = 1-10, 12, 14, and 16

Figure 4.7: General chemical structure of unsymmetrical derivatives

4.2. Experimental Section

4.2.1 Materials and Measurements

All the chemicals and solvents were purchased from Sigma Aldrich. The following sources were used: n-alkyl bromide, 4-n-hydroxy acetanilide from Spectrochem Pvt. Ltd., 3-ethoxy-4-hydroxybezaldehyde from sigma Aldrich, pyridine, potassium hydroxide, p-hydroxybenzoic acid, thionyl chloride, absolute alcohol, and glacial acetic acid from Lobachemie Pvt. Ltd. Aluminum silica gel plates (Merck 60 F245) were used for Thin Layer Chromatography (TLC), which was examined under a UV lamp. FT-IR spectra were obtained using a Perkin Elmer Spectrum Two. Avance Bruker 400 spectrophotometer (400 MHz & 150 MHz, respectively) was used to record ^{1}H NMR and ^{13}C NMR spectra data. TMS was used as an internal standard, and the solvent was deuterated chloroform ($CDCl_3$). The thermal behavior of prepared compounds was studied using a Nikon Eclipse Ci-Pol microscope (Japan) outfitted with a Linkam heating stage (to ascertain the transition temperatures of prepared compounds), platinum pans for differential scanning calorimetry (DSC-822, Mettler Toledo with Stare software), 4-5 mg of sample with 30–40 mL min^{-1} nitrogen gas inert atmosphere, and a heating rate of 10 °C min^{-1}. To assess the thermal stability, a sample of about 2-3 mg was placed in a

thermogravimetric analyzer (TGA-50, Shimadzu Japan). The elemental analysis was performed using a Thermo Finnigan (Flash 1112 series EA) CHN analyzer. A spectrofluorometer, the Shimadzu RF-6000 (Japan), was used to examine the photoluminescence study.

4.2.2 Synthesis and Characterization

4.2.2.1 Synthesis of 4-n-alkoxybenzoic acid (1a-1m) [79]

In 40 mL of ethanol, p-hydroxybenzoic acid (0.1 mol), an alkyl halide (0.12 mol), and potassium hydroxide were dissolved. The mixture was then refluxed for 4-5 h. To hydrolyze the ester produced, 10% aqueous KOH solution (25 mL) was added and reflux was carried out for 2 h. To precipitate the formed acid, the prepared solution was cooled and acidified with 1:1 dil. HCl. By employing the proper solvent and the recrystallization process, compounds were purified until constant transition temperatures were attained.

4.2.2.2 Synthesis of 2'-ethoxy-4'-formylphenyl 4-alkoxybenzoate (2a-2m)

4-n-alkoxy benzoic acid reacts with an excess of thionyl chloride, 4-n alkoxy benzoyl chloride was formed. The excess thionyl chloride was removed by distillation. After treating the resulting acid chloride with 3-ethoxy-4-hydroxybenzaldehyde and heating it for one hour in a water bath, 2'-ethoxy-4'-formylphenyl 4-alkoxybenzoate was formed.

4.2.2.3 Synthesis of 4-n-decyloxyaniline (3a-3m) [80]

4-n-Hydroxy acetanilide (0.1 mol), anhydrous potassium carbonate (0.1 mol), and dry acetone (60 mL) were heated at 70-80 °C and to the warm solution, the appropriate alkyl halide was added dropwise for 1 h. The mixture was refluxed with continuous stirring at 70-80 °C for 8-10 h. The obtained product was diluted with cold water. The mixture obtained was filtered, cleaned with water, and directly used for hydrolysis under appropriate conditions. Yield obtained: 80-85%. Reported Melting Point: 65.2 °C.

4.2.2.4 Synthesis of 4'-(4''-decyloxyphenyliminomethyl)-2'-ethoxyphenyl-4-alkoxybenzoate (4a-4m) [Series-I]

2'-ethoxy-4'-formylphenyl-4-alkoxybenzoate (0.1 mol) was treated with 4-n-decyloxyaniline (0.1 mol) using absolute alcohol (10-12 mL) and glacial acetic acid as a catalyst. Reflux was carried out for 3 h. The product obtained was recrystallized from ethanol.

4'-(4''-decyloxyphenyliminomethyl)-2'-ethoxyphenyl-4-methoxybenzoate (4a)

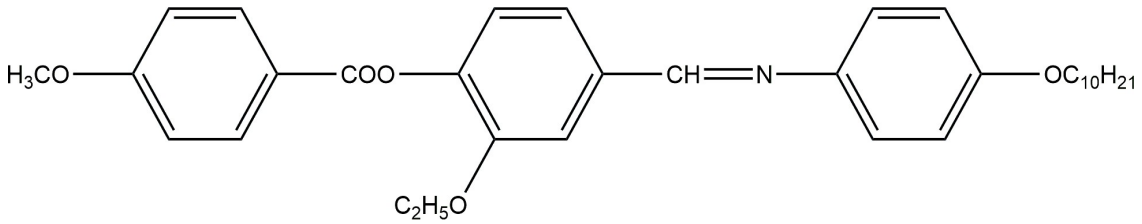

Light yellow crystal, yield 76.30%. **FT-IR** (cm^{-1}): 2925, 2857 (C-H, aliphatic), 1750 (C=O in ester), 1624 (-C=N-), 1579, 1515, 1478 (-C=C-, aromatic), 1295, 1256 (R-O-Ar, ether). **^{1}H NMR** (400 MHz, $CDCl_3$) δ (ppm): 7.30 (s, 1H, Ar-H), 8.47 (s, 1H, -CH=N-), 6.98-6.95 (d, 4H, J = 8.4 Hz, Ar-H), 7.30-7.01 (d, 4H, J = 8.8 Hz, Ar-H), 8.21-7.22 (d, 2H, J = 8.4 Hz, Ar-H), 1.86-1.36 (m, 16H,-CH_2-CH_2-), 4.20-4.02 (m, 4H, -Ar-O-CH_2-), 1.42, 0.89 (t, 6H, -CH_2-CH_3), 3.81 (s, 3H, -OCH_3). **^{13}C NMR** (100 MHz, $CDCl_3$) δ (ppm): 164.3 (-C=O), 159.8 (-CH=N-), 157.8, 157.4, 157.3 (Ar-C-O), 144.6 (-C-N), 142.7, 134.1, 133.3, 124.0, 121.6, 120.1, 119.4, 114.9, 114.2, 111.6 (Ar-C), 68.3, 64.6, 63.8 (Ar-O-CH_2-), 31.9, 29.6, 29.1, 29.0, 26.1, 22.7 (-CH_2-CH_2-), 14.8, 14.1 (-CH_2-CH_3).

4'-(4''-decyloxyphenyliminomethyl)-2'-ethoxyphenyl-4-ethoxybenzoate (4b)

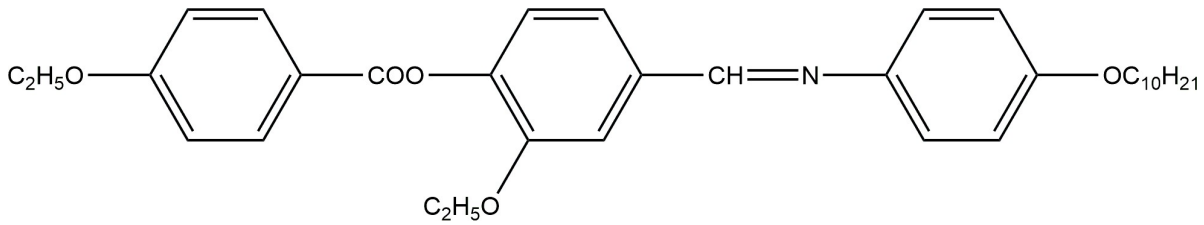

Light yellow crystal, yield 75.11%. **FT-IR** (cm^{-1}): 2980, 2922, 2850 (C-H, aliphatic), 1728 (C=O in ester), 1606 (-C=N-), 1579, 1514, 1475 (-C=C-, aromatic), 1294 (R-O-Ar, ether). **^{1}H NMR** (400 MHz, $CDCl_3$) δ (ppm): 7.40 (s, 1H, Ar-H), 8.46 (s, 1H, -CH=N-), 6.99-6.94 (d, 4H, J = 8.4 Hz, Ar-H), 7.39-7.28 (d, 4H, J = 8.8 Hz, Ar-H), 8.20-7.73 (d, 2H, J = 8.4 Hz, Ar-H), 1.85-1.30 (m, 16H,-CH_2-CH_2-), 4.20-4.01 (m, 4H, -Ar-O-CH_2-), 4.21 (t, 2H, Ar-O-CH_2-), 1.47, 0.89 (t, 9H, -CH_2-CH_3). **^{13}C NMR** (100 MHz, $CDCl_3$) δ (ppm): 164.2 (-C=O), 157.8 (-CH=N-), 157.8, 157.4, 157.3 (Ar-C-O), 144.5 (-C-N), 142.9, 135.1, 132.3, 123.0, 122.6, 122.1, 121.4, 114.9, 114.2, 111.6 (Ar-C), 68.2, 64.5, 63.7 (Ar-O-CH_2-), 31.8, 29.5, 29.3, 29.2, 26.0, 22.6 (-CH_2-CH_2-), 14.6, 14.0 (-CH_2-CH_3).

4'-(4''-decyloxyphenyliminomethyl)-2'-ethoxyphenyl-4-propoxybenzoate (4c)

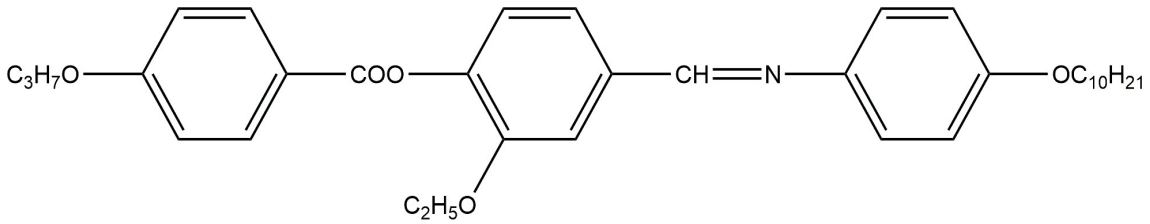

Creamy crystal, yield 77.58%. **FT-IR** (cm^{-1}): 2928, 2925, 2853, 2798 (C-H, aliphatic), 1760 (C=O in ester), 1628 (-C=N-), 1576, 1512, 1475 (-C=C-, aromatic), 1294, 1258 (R-O-Ar, ether). **^{1}H NMR** (400 MHz, $CDCl_3$) δ (ppm): 7.41 (s, 1H, Ar-H), 8.48 (s, 1H, -CH=N-), 6.98-6.93 (d, 4H, J = 8.4 Hz, Ar-H), 7.40-7.24 (d, 4H, J = 8.8 Hz, Ar-H), 8.28-7.76 (d, 2H, J = 8.4 Hz, Ar-H), 1.89-1.31 (m, 18H,-CH_2-CH_2-), 4.19-4.03 (m, 4H, -Ar-O-CH_2-), 4.20 (t, 2H, Ar-O-CH_2-), 1.48, 0.88 (t, 9H, -CH_2-CH_3). **^{13}C NMR** (100 MHz, $CDCl_3$) δ (ppm): 164.1 (-C=O), 159.8 (-CH=N-), 157.8, 157.4, 157.3 (Ar-C-O), 144.8 (-C-N), 142.9, 136.1, 131.3, 125.0, 121.6, 121.1, 121.0, 114.9, 114.3, 114.2, 111.6 (Ar-C), 68.6, 64.6, 63.8 (Ar-O-CH_2-), 31.8, 29.5, 29.6, 29.3, 26.1, 22.7 (-CH_2-CH_2-), 14.7, 14.2 (-CH_2-CH_3).

4'-(4''-decyloxyphenyliminomethyl)-2'-ethoxyphenyl-4-butoxybenzoate (4d)

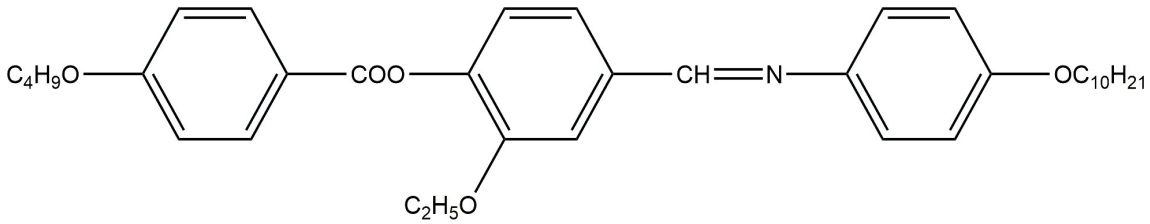

White crystal, yield 78.15%. **FT-IR** (cm^{-1}): 2953, 2928, 2868, 2852 (C-H, aliphatic), 1768 (C=O in ester), 1732 (-C=N-), 1475, 1512, 1581 (-C=C-, aromatic), 1255 (R-O-Ar, ether). **^{1}H NMR** (400 MHz, $CDCl_3$) δ (ppm): 7.40 (s, 1H, Ar-H), 8.46 (s, 1H, -CH=N-), 7.01-6.94 (d, 4H, J = 8.4 Hz, Ar-H), 7.37-7.25 (d, 4H, J = 8.8 Hz, Ar-H), 8.20-7.38 (d, 2H, J = 2.4 Hz, Ar-H), 1.87-1.30 (m, 20H, -CH_2-CH_2-), 4.18-4.01 (t, 4H, Ar-O-CH_2-), 4.19 (m, 2H, Ar-O-CH_2-), 1.24, 0.90, 0.89 (t, 9H, -CH_2-CH_3). **^{13}C NMR** (100 MHz, $CDCl_3$) δ (ppm): 164.5 (-C=O), 160.0 (-CH=N-), 157.8, 157.4, 157.3 (Ar-C-O), 144.9 (-C-N), 137.1, 132.3, 126.0, 122.6, 122.1, 121.2, 121.1 , 114.9, 114.6, 114.3, 111.7 (Ar-C), 68.6, 64.6, 63.8 (Ar-O-CH_2-), 31.9, 31.8, 29.8, 29.6, 29.5, 29.3, 26.1, 22.7, 21.9 (-CH_2-CH_2-), 14.8, 14.7, 14.2 (-CH_2-CH_3).

4'-(4''-decyloxyphenyliminomethyl)-2'-ethoxyphenyl-4-pentyloxybenzoate (4e)

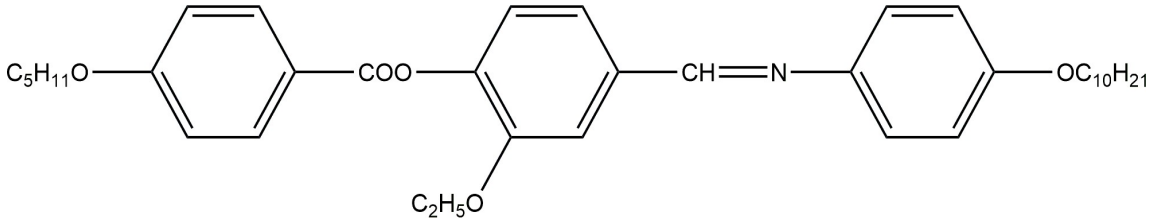

Light yellow crystal, yield 76.10%. **FT-IR** (cm^{-1}): 2982, 2943, 2922, 2848 (C-H, aliphatic), 1735 (C=O in ester), 1626 (-C=N-), 1585, 1510, 1475 (-C=C-, aromatic), 1273, 1255 (R-O-Ar, ether). **^{1}H NMR** (400 MHz, $CDCl_3$) δ (ppm): 7.40 (s, 1H, Ar-H), 8.46 (s, 1H, -CH=N-), 7.24-6.96 (d, 4H, J = 8.4 Hz, Ar-H), 7.38-7.25 (d, 4H, J = 8.8 Hz, Ar-H), 8.19-7.39 (d, 2H, Ar-H), 4.18-4.01 (t, 4H, Ar-O-CH_2-), 4.21 (m, 2H, Ar-O-CH_2-) 1.87-1.30 (m, 22H, -CH_2-CH_2-), 1.27-0.90 (t, 9H, -CH_2-CH_3). **^{13}C NMR** (100 MHz, $CDCl_3$) δ (ppm): 164.3 (-C=O), 159.8 (-CH=N-), 157.8, 157.4, 157.3 (Ar-C-O), 144.6 (-C-N), 142.7, 134.1, 133.3, 124.0, 121.6, 120.1, 119.4, 114.9, 114.2, 111.6 (Ar-C), 68.3, 64.6, 63.8 (Ar-O-CH_2-), 31.9, 31.8, 29.8, 29.7, 29.6, 29.1, 29.0, 27.9, 26.1, 22.7 (-CH_2-CH_2-), 14.8, 14.5, 14.1 (-CH_2-CH_3).

4'-(4''-decyloxyphenyliminomethyl)-2'-ethoxyphenyl-4-hexyloxybenzoate (4f)

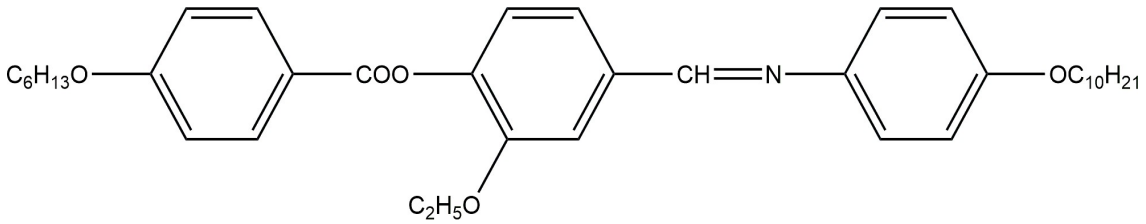

Yellow crystal, yield 77.48%. **FT-IR** (cm^{-1}): 2983, 2922, 2852 (C-H, aliphatic), 1730 (C=O in ester), 1624 (-C=N-), 1467, 1508, 1579 (-C=C-, aromatic), 1274, 1249 (R-O-Ar, ether). **^{1}H NMR** (400 MHz, $CDCl_3$) δ (ppm): 7.39 (s, 1H, Ar-H), 8.46 (s, 1H, -CH=N-), 7.38-7.28 (d, 4H, J = 8.4 Hz, Ar-H), 7.27-7.24 (d, 4H, J = 8.8 Hz, Ar-H), 7.01-6.94 (d, 2H, Ar-H), 4.19-4.01 (t, 4H, Ar-O-CH_2-), 4.21 (m, 2H, Ar-O-CH_2-), 1.86-1.30 (m, 24H, -CH_2-CH_2-), 1.27-0.90 (t, 9H, -CH_2-CH_3). **^{13}C NMR** (100 MHz, $CDCl_3$) δ (ppm): 164.1 (-C=O), 159.8 (-CH=N-), 157.8, 157.4, 157.3 (Ar-C-O), 144.5 (-C-N), 142.9, 135.1, 132.3, 123.0, 122.6, 122.1, 121.4, 114.9, 114.2, 111.6 (Ar-C), 68.2, 64.5, 63.7 (Ar-O-CH_2-), 31.8, 31.7, 31.2, 29.5, 29.4, 29.3, 29.2, 27.9, 26.0, 22.8, 22.7, 22.6 (-CH_2-CH_2-), 14.8, 14.6, 14.0 (-CH_2-CH_3).

4'-(4''-decyloxyphenyliminomethyl)-2'-ethoxyphenyl-4-heptyloxybenzoate (4g)

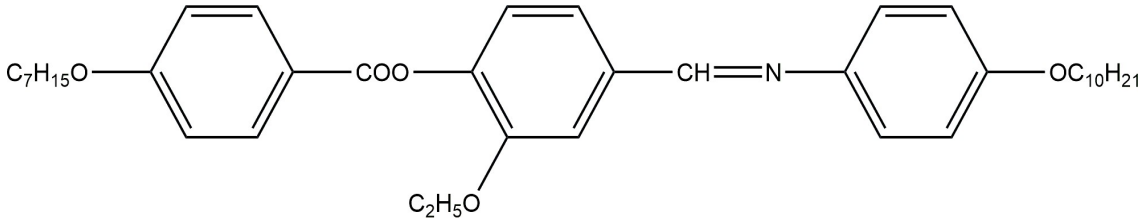

White crystal, yield 77.50%. **FT-IR** (cm^{-1}): 2928, 2851, 2848 (C-H, aliphatic), 1734 (C=O in ester), 1624 (-C=N-), 1575, 1534, 1475 (-C=C-, aromatic), 1290, 1250 (R-O-Ar, ether). **^{1}H NMR** (400 MHz, $CDCl_3$) δ (ppm): 7.40 (s, 1H, Ar-H), 8.47 (s, 1H, -CH=N-), 7.39-7.27 (d, 4H, J = 8.4 Hz, Ar-H), 7.26-7.22 (d, 4H, J = 8.8 Hz, Ar-H), 7.01-6.94 (d, 2H, Ar-H), 4.20-4.02 (t, 4H, Ar-O-CH_2-), 4.21 (m, 2H, Ar-O-CH_2-), 1.88-1.31 (m, 26H, -CH_2-CH_2-), 0.92-0.90 (t, 9H, -CH_2-CH_3). **^{13}C NMR** (100 MHz, $CDCl_3$) δ (ppm): 164.1 (-C=O), 159.8 (-CH=N-), 157.8, 157.4, 157.3 (Ar-C-O), 144.8 (-C-N), 142.9, 136.1, 131.3, 125.0, 121.6, 121.1, 121.0, 114.9, 114.3, 114.2, 111.6 (Ar-C), 68.6, 64.6, 63.8 (Ar-O-CH_2-), 31.8, 31.7, 31.5, 29.6, 29.5, 29.3, 29.1, 26.1, 26.0, 22.8, 22.7, 21.8, 21.7 (-CH_2-CH_2-), 14.7, 14.6, 14.1 (-CH_2-CH_3).

4'-(4''-decyloxyphenyliminomethyl)-2'-ethoxyphenyl-4-octyloxybenzoate (4h)

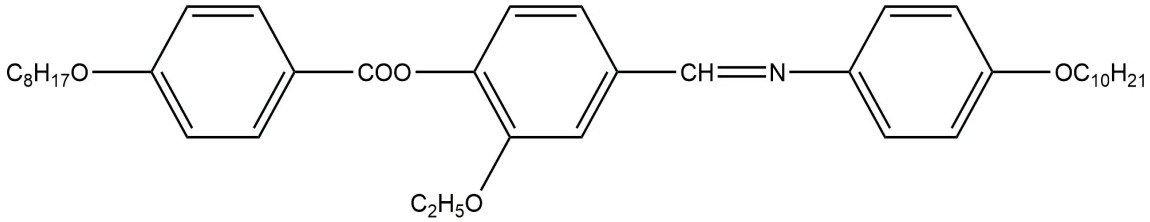

Light yellow crystal, yield 75.06%. **FT-IR** (cm^{-1}): 2951, 2922, 2870, 2850 (C-H, aliphatic), 1724 (C=O in ester), 1624 (-C=N-), 1577, 1510, 1467 (-C=C-, aromatic), 1292, 1292, 1257 (R-O-Ar, ether). **^{1}H NMR** (400 MHz, $CDCl_3$) δ (ppm): 7.40 (s, 1H, Ar-H), 8.46 (s, 1H, -CH=N-), 7.38-7.26 (d, 4H, J = 8.4 Hz, Ar-H), 7.01-6.99 (d, 4H, J = 8.8 Hz, Ar-H), 6.96-6.94 (d, 2H, Ar-H), 4.22 (m, 2H, Ar-O-CH_2-), 4.21-3.93 (t, 4H, Ar-O-CH_2-), 1.88-1.24 (m, 28H, -CH_2-CH_2-), 1.22 (t, 9H, -CH_2-CH_3). **^{13}C NMR** (100 MHz, $CDCl_3$) δ (ppm): 164.3 (-C=O), 157.8 (-CH=N-), 157.6, 157.4, 157.3 (Ar-C-O), 144.5 (-C-N), 142.9, 135.1, 132.3, 123.0, 122.6, 122.1, 121.3, 114.9, 114.2, 114.1, 111.6 (Ar-C), 68.6, 64.6, 63.8 (Ar-O-CH_2-), 31.8, 31.7, 29.5, 29.3, 29.2, 29.0, 26.0, 25.9, 22.6, 22.6, 22.5, 21.9, 21.8, 21.7 (-CH_2-CH_2-), 14.8, 14.6, 14.1 (-CH_2-CH_3).

4'-(4''-decyloxyphenyliminomethyl)-2'-ethoxyphenyl-4-nonyloxybenzoate (4i)

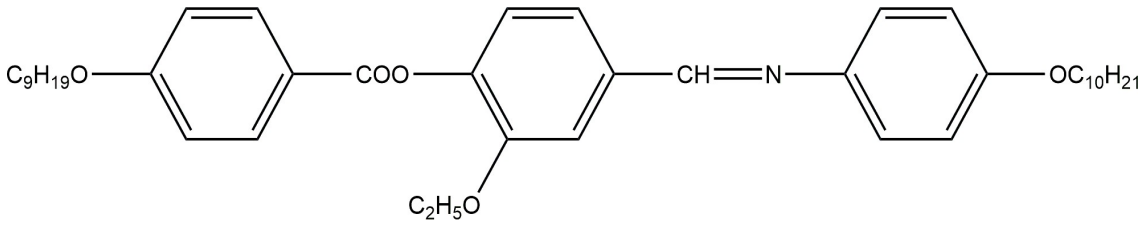

Light brown crystal, yield 78.51%. **FT-IR** (cm^{-1}): 2922, 2853 (C-H, aliphatic), 1768 (C=O in ester), 1620 (-C=N-), 1578, 1475, 1450 (-C=C-, aromatic), 1294, 1251 (R-O-Ar, ether). **^{1}H NMR** (400 MHz, $CDCl_3$) δ (ppm): 7.42 (s, 1H, Ar-H), 8.44 (s, 1H, -CH=N-), 7.39-7.25 (d, 4H, J = 8.4 Hz, Ar-H), 7.00-6.96 (d, 4H, J = 8.8 Hz, Ar-H), 6.95-6.92 (d, 2H, Ar-H), 4.21 (m, 2H, Ar-O-CH_2-), 4.20-3.93 (t, 4H, Ar-O-CH_2-), 1.89-1.23 (m, 30H, -CH_2-CH_2-), 1.21 (t, 9H, -CH_2-CH_3). **^{13}C NMR** (100 MHz, $CDCl_3$) δ (ppm): 164.1 (-C=O), 159.8 (-CH=N-), 157.8, 157.4, 157.3 (Ar-C-O), 144.5 (-C-N), 142.9, 135.1, 132.3, 123.0, 122.6, 122.1, 121.4, 114.9, 114.2, 111.6 (Ar-C), 68.2, 64.5, 63.7 (Ar-O-CH_2-), 31.8, 31.7, 31.2, 29.5, 29.4, 29.3, 29.2, 27.9, 26.0, 25.9, 25.8, 25.7, 22.8, 22.7, 22.6 (-CH_2-CH_2-), 14.8, 14.6, 14.0 (-CH_2-CH_3).

4'-(4''-decyloxyphenyliminomethyl)-2'-ethoxyphenyl-4-decyloxybenzoate (4j)

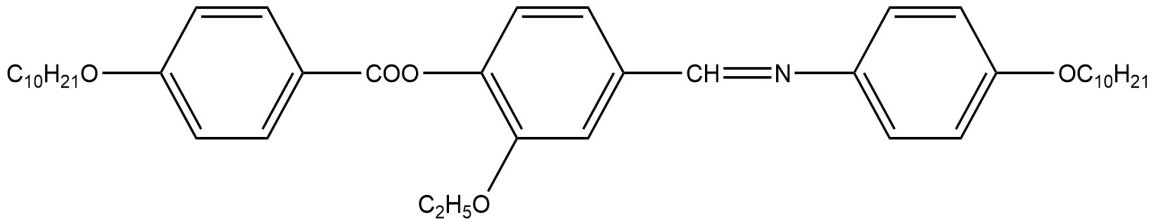

Colourless needle-like crystal, yield 79.73%. **FT-IR** (cm^{-1}): 2922, 2853 (C-H, aliphatic), 1768 (C=O in ester), 1626 (-C=N-), 1575, 1534, 1478 (-C=C-, aromatic), 1292, 1251 (R-O-Ar, ether). **^{1}H NMR** (400 MHz, $CDCl_3$) δ (ppm): 7.40 (s, 1H, Ar-H), 8.46 (s, 1H, -CH=N-), 7.40-7.22 (d, 4H, J = 8.4 Hz, Ar-H), 7.01-6.94 (d, 4H, J = 8.8 Hz, Ar-H), 6.93-6.90 (d, 2H, Ar-H), 4.21 (m, 2H, Ar-O-CH_2-), 4.19-3.93 (t, 4H, Ar-O-CH_2-), 1.88-1.24 (m, 32H, -CH_2-CH_2-), 1.21 (t, 9H, -CH_2-CH_3). **^{13}C NMR** (100 MHz, $CDCl_3$) δ (ppm): 164.3 (-C=O), 157.8 (-CH=N-), 157.6, 157.4, 157.3 (Ar-C-O), 144.5 (-C-N), 142.9, 135.1, 132.3, 123.0, 122.6, 122.1, 121.3, 114.9, 114.2, 114.1, 111.6 (Ar-C), 68.6, 64.6, 63.8 (Ar-O-CH_2-), 31.8, 31.7, 29.5, 29.3, 29.2, 29.0, 26.0, 25.9, 22.6, 22.6, 22.5, 22.4, 22.3, 21.9, 21.8, 21.7 (-CH_2-CH_2-), 14.8, 14.6, 14.1 (-CH_2-CH_3).

4'-(4''-decyloxyphenyliminomethyl)-2'-ethoxyphenyl-4-dodecyloxybenzoate (4k)

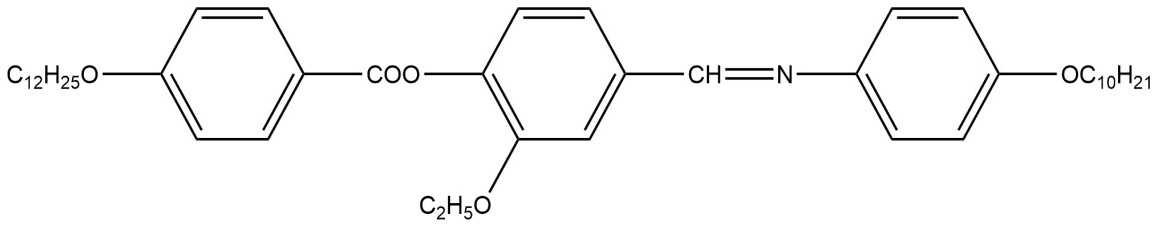

Light yellow crystal, yield 80.51%. **FT-IR** (cm^{-1}): 2922, 2853 (C-H, aliphatic), 1768 (C=O in ester), 1626 (-C=N-), 1506 (-C=C-, aromatic), 1292, 1251 (R-O-Ar, ether). **^{1}H NMR** (400 MH_Z, $CDCl_3$) δ (ppm): 7.41 (s, 1H, Ar-H), 8.48 (s, 1H, -CH=N-), 7.40-7.22 (d, 4H, J = 8.4 Hz, Ar-H), 7.01-6.94 (d, 4H, J = 8.8 Hz, Ar-H), 6.93-6.91 (d, 2H, Ar-H), 4.21 (m, 2H, Ar-O-CH_2-), 4.20-3.94 (t, 4H, Ar-O-CH_2-), 1.89-1.26 (m, 36H, -CH_2-CH_2-), 1.20 (t, 9H, -CH_2-CH_3). **^{13}C NMR** (100 MHz, $CDCl_3$) δ (ppm): 164.1 (-C=O), 159.8 (-CH=N-), 157.8, 157.4, 157.3 (Ar-C-O), 144.5 (-C-N), 142.9, 135.1, 132.3, 123.0, 122.6, 122.1, 121.4, 114.9, 114.2, 111.6 (Ar-C), 68.2, 64.5, 63.7 (Ar-O-CH_2-), 31.8, 31.7, 31.2, 29.5, 29.4, 29.3, 29.2, 27.9, 26.0, 25.9, 25.8, 25.7, 25.6, 25.4, 25.3, 22.8, 22.7, 22.6 (-CH_2-CH_2-), 14.8, 14.6, 14.0 (-CH_2-CH_3).

4'-(4''-decyloxyphenyliminomethyl)-2'-ethoxyphenyl-4-tetradecyloxybenzoate (4l)

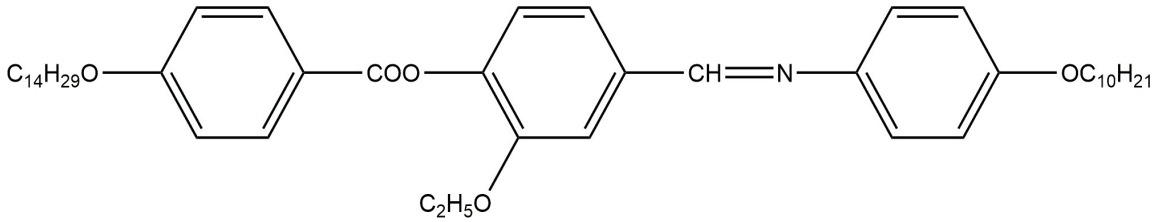

Yellow crystal, yield 79.33%. **FT-IR** (cm^{-1}): 2924, 2851 (C-H, aliphatic), 1768 (C=O in ester), 1600 (-C=N-), 11578, 1523, 1475 (-C=C-, aromatic), 1292, 1251 (R-O-Ar, ether). **^{1}H NMR** (400 MH_Z, $CDCl_3$) δ (ppm): 7.40 (s, 1H, Ar-H), 8.46 (s, 1H, -CH=N-), 7.42-7.21 (d, 4H, J = 8.4 Hz, Ar-H), 7.03-6.93 (d, 4H, J = 8.8 Hz, Ar-H), 6.92-6.89 (d, 2H, Ar-H), 4.20 (m, 2H, Ar-O-CH_2-), 4.19-3.93 (t, 4H, Ar-O-CH_2-), 1.88-1.27 (m, 40H, -CH_2-CH_2-), 1.21 (t, 9H, -CH_2-CH_3). **^{13}C NMR** (100 MHz, $CDCl_3$) δ (ppm): 164.3 (-C=O), 157.8 (-CH=N-), 157.6, 157.4, 157.3 (Ar-C-O), 144.5 (-C-N), 142.9, 135.1, 132.3, 123.0, 122.6, 122.1, 121.3, 114.9, 114.2, 114.1, 111.6 (Ar-C), 68.6, 64.6, 63.8 (Ar-O-CH_2-), 31.8, 31.7, 29.5, 29.3, 29.2, 29.0, 26.0, 25.9, 22.6, 22.6, 22.5, 22.4, 22.3, 22.2, 21.9, 21.9, 21.8, 21.7 (-CH_2-CH_2-), 14.8, 14.6, 14.1 (-CH_2-CH_3).

4'-(4''-decyloxyphenyliminomethyl)-2'-ethoxyphenyl-4-hexadecyloxybenzoate (4m)

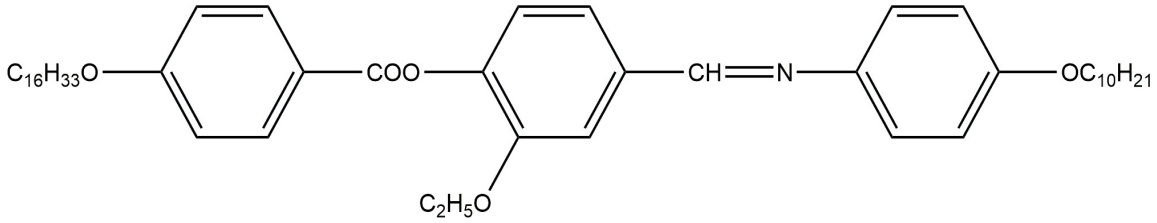

White needle-like crystal, yield 76.14%. **FT-IR** (cm^{-1}): 2924, 2851 (C-H, aliphatic), 1768 (C=O in ester), 1626 (-C=N-), 1575, 1512, 1478 (-C=C-, aromatic), 1296, 1250 (R-O-Ar, ether). **^{1}H NMR** (400 MH_Z, $CDCl_3$) δ (ppm): 7.42 (s, 1H, Ar-H), 8.48 (s, 1H, -CH=N-), 7.42-7.21 (d, 4H, J = 8.4 Hz, Ar-H), 7.03-6.93 (d, 4H, J = 8.8 Hz, Ar-H), 6.92-6.89 (d, 2H, Ar-H), 4.20 (m, 2H, Ar-O-CH_2-), 4.19-3.93 (t, 4H, Ar-O-CH_2-), 1.88-1.27 (m, 44H, -CH_2-CH_2-), 1.21 (t, 9H, -CH_2-$\underline{C}H_3$). **^{13}C NMR** (100 MHz, $CDCl_3$) δ (ppm): 164.3 (-C=O), 157.8 (-CH=N-), 157.6, 157.4, 157.3 (Ar-C-O), 144.5 (-C-N), 142.9, 135.1, 132.3, 123.0, 122.6, 122.1, 121.3, 114.9, 114.2, 114.1, 111.6 (Ar-C), 68.6, 64.6, 63.8 (Ar-O-CH_2-), 31.8, 31.7, 29.5, 29.3, 29.2, 29.0, 26.0, 25.9, 22.6, 22.6, 22.5, 22.4, 22.3, 21.9, 21.8, 21.7 (-CH_2-CH_2-), 14.8, 14.6, 14.1 (-CH_2-$\underline{C}H_3$).

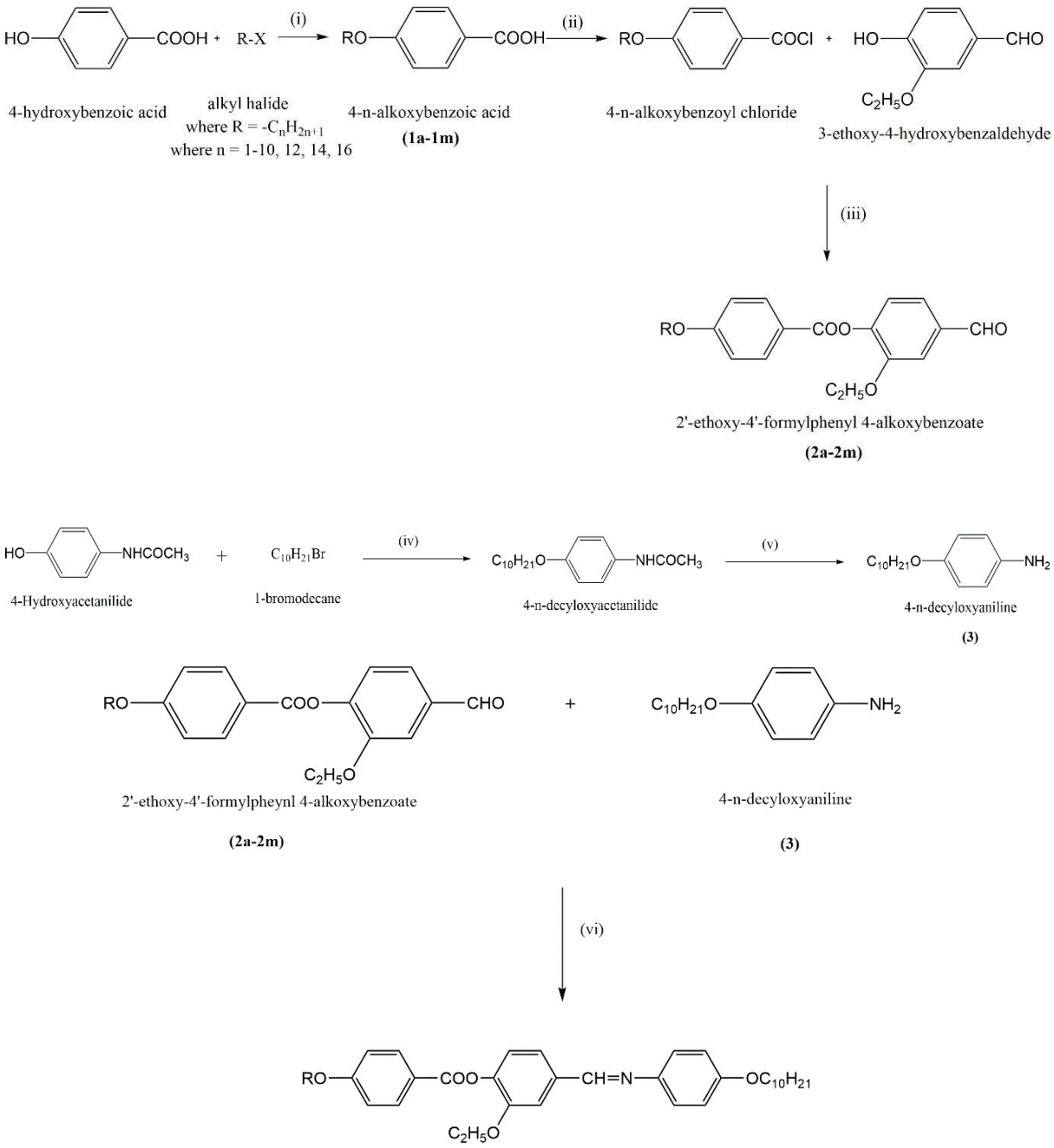

Series-I (4a-4m)

where R = -C_nH_{2n+1}, n = 1-10, 12, 14, 16

Scheme 4.1: The synthetic procedure of Unsymmetrical homologous series. Reagents and conditions: (i) RBr, KOH, EtOH, reflux 8-10 h; (ii) $SOCl_2$, pyridine, heat; 2 h (iii) pyridine, heat on the water bath, 1 h; (iv) & (v) anhydrous potassium carbonate, dry acetone, alkyl halide, 70-80 °C, 8-10 h. (vi) Few drops of glacial AcOH, absolute EtOH, reflux 3-4 h.

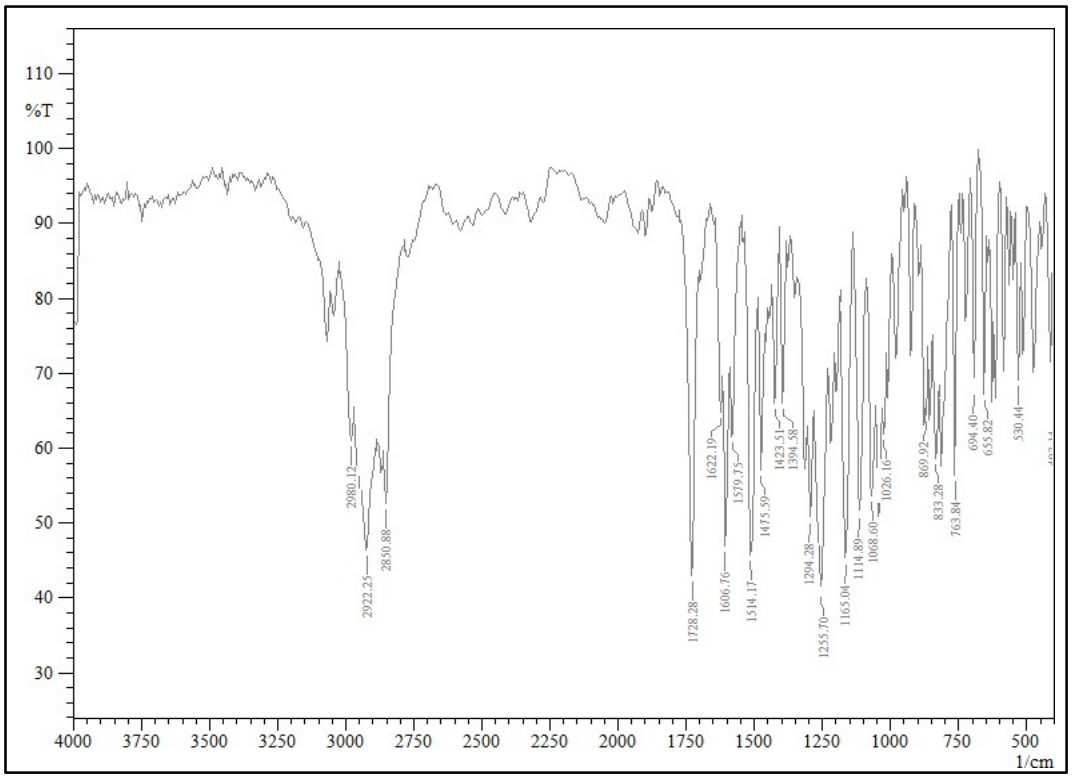

Figure 4.8: FT-IR spectra of 4'-(4"-decyloxyphenyliminomethyl)-2'-ethoxyphenyl-4-ethoxybenzoate (4b)

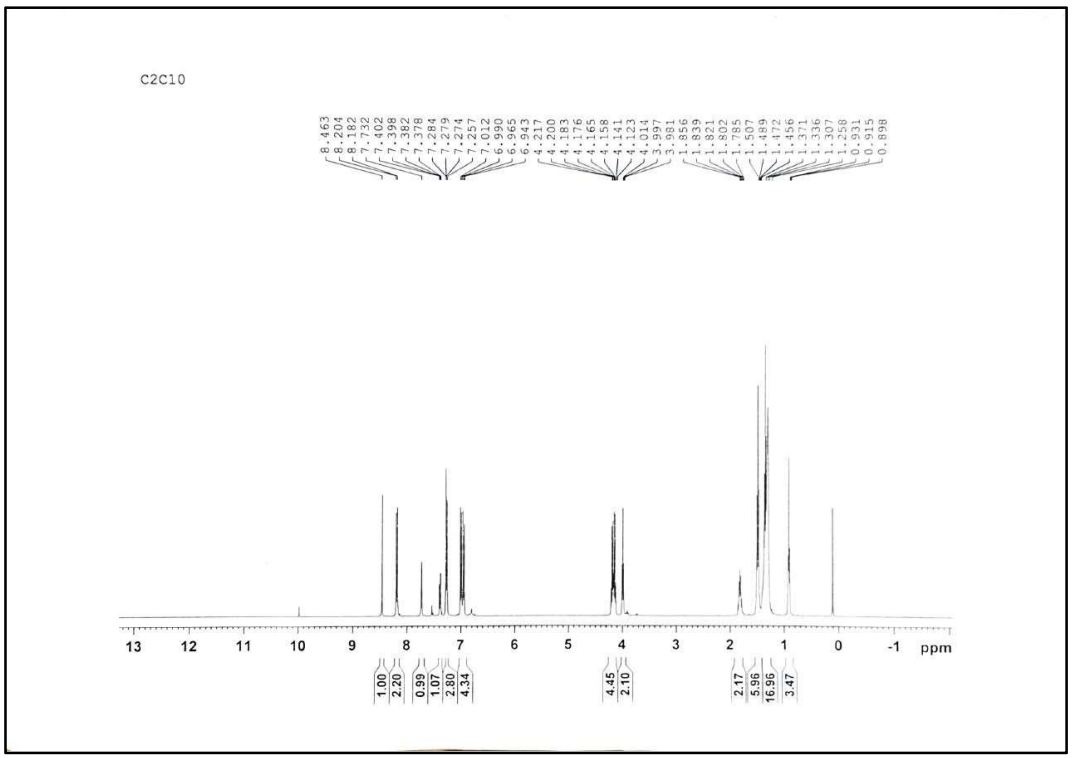

Figure 4.9: ^{1}H NMR spectra of 4'-(4"-decyloxyphenyliminomethyl)-2'-ethoxyphenyl-4-ethoxybenzoate (4b)

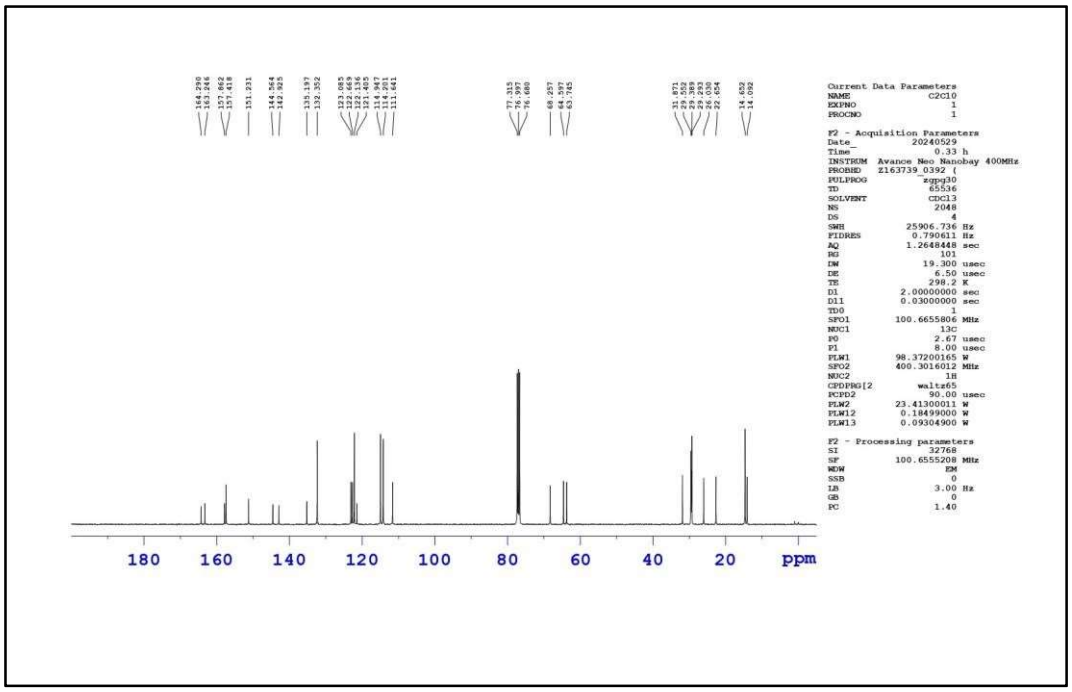

Figure 4.10: ^{13}C NMR spectra of 4'-(4''-decyloxyphenyliminomethyl)-2'-ethoxyphenyl-4-ethoxybenzoate (4b)

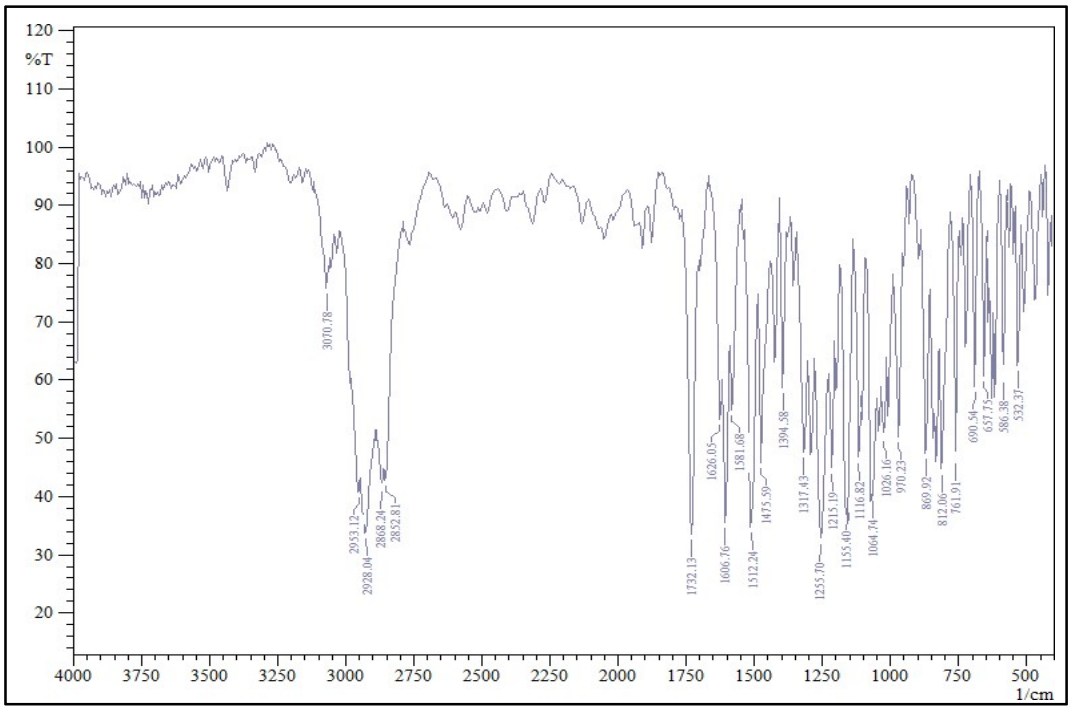

Figure 4.11: FT-IR spectra of 4'-(4''-decyloxyphenyliminomethyl)-2'-ethoxyphenyl-4-butoxybenzoate (4d)

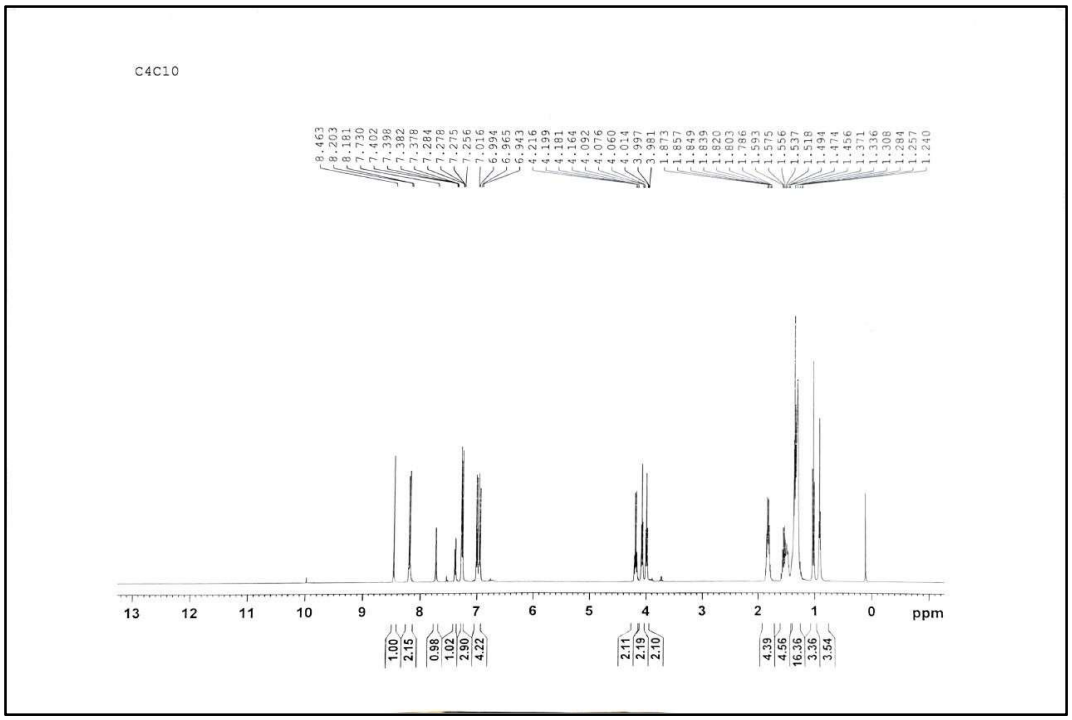

Figure 4.12: ^{1}H NMR spectra of 4'-(4''-decyloxyphenyliminomethyl)-2'-ethoxyphenyl-4-butoxybenzoate (4d)

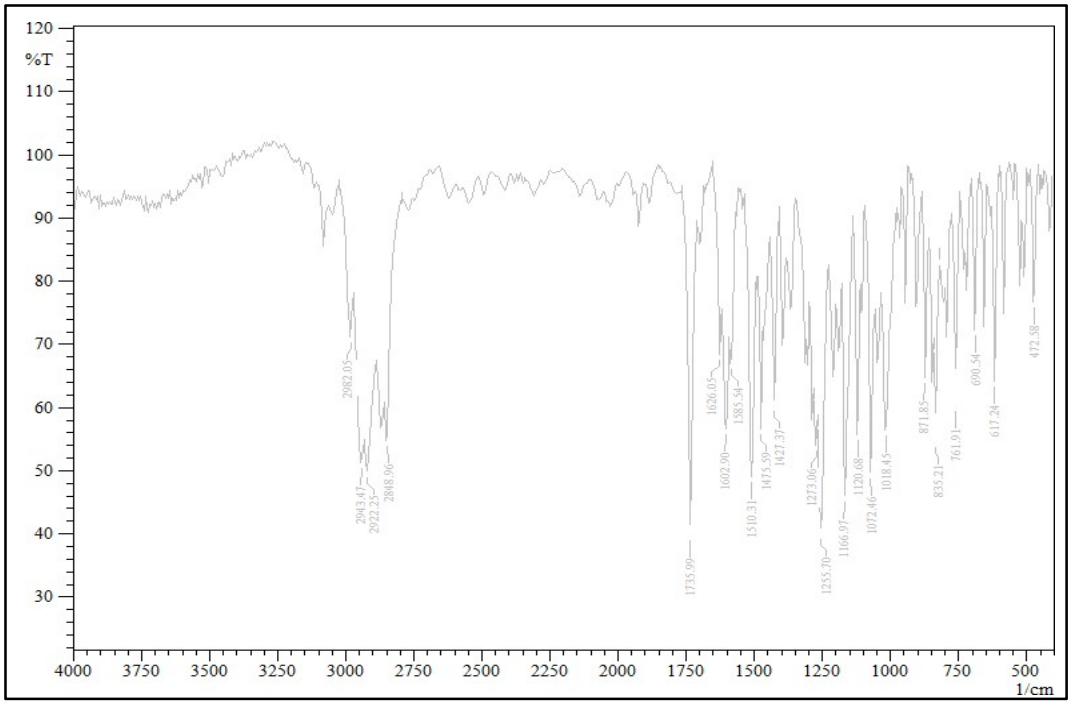

Figure 4.13: FT-IR spectra of 4'-(4''-decyloxyphenyliminomethyl)-2'-ethoxyphenyl-4-pentyloxybenzoate (4e)

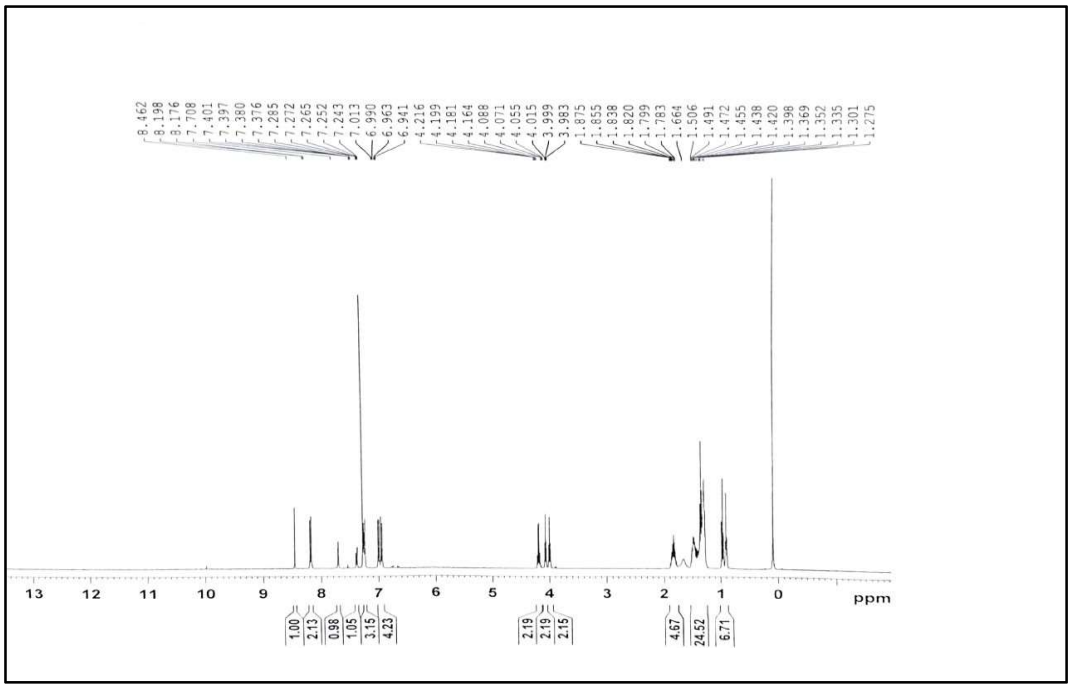

Figure 4.14: ^{1}H NMR spectra of 4'-(4"-decyloxyphenyliminomethyl)-2'-ethoxyphenyl-4-pentyloxybenzoate (4e)

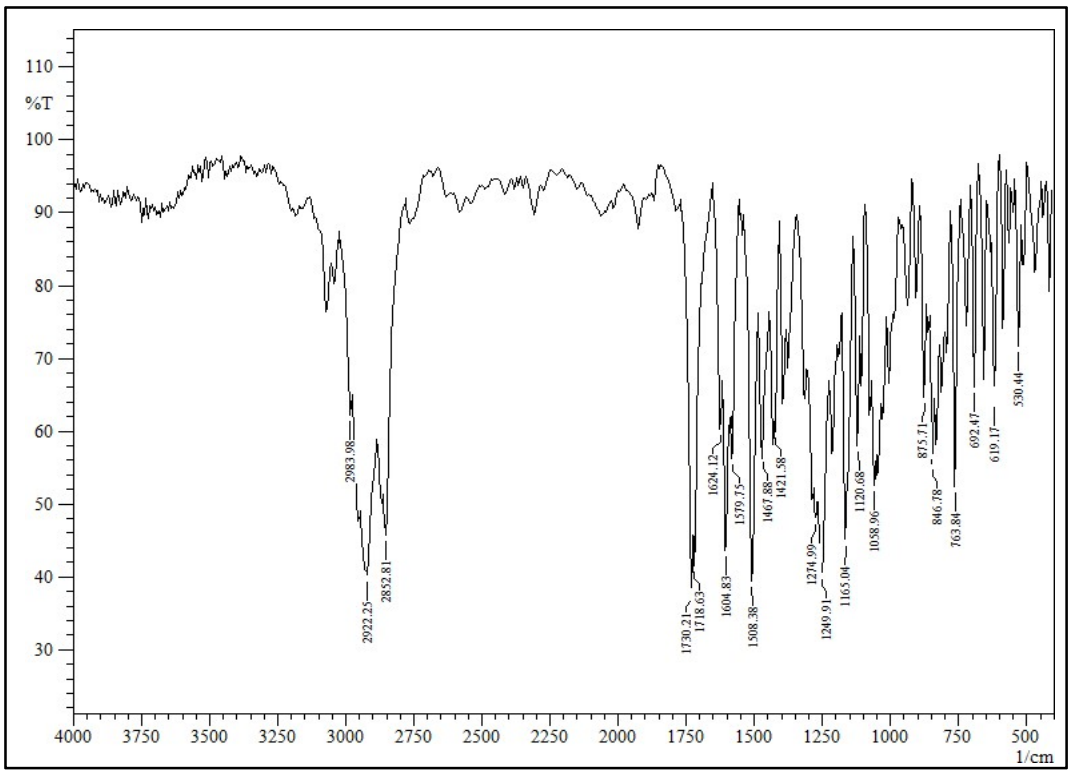

Figure 4.15: FT-IR spectra of 4'-(4"-decyloxyphenyliminomethyl)-2'-ethoxyphenyl-4-hexyloxybenzoate (4f)

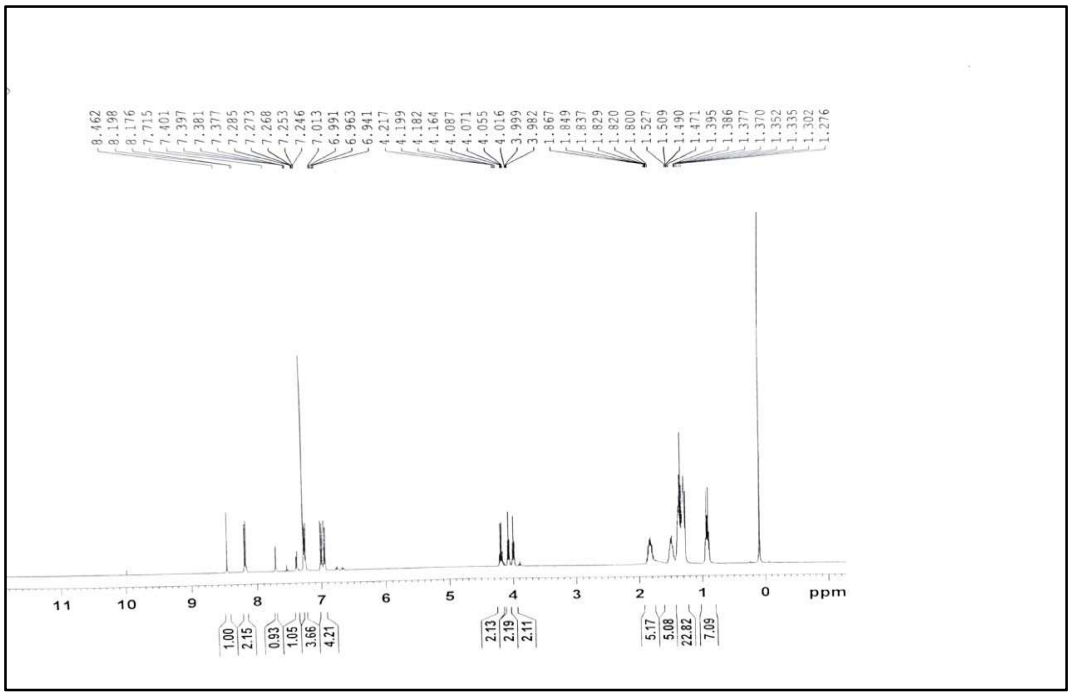

Figure 4.16: ^{1}H NMR spectra of 4'-(4''-decyloxyphenyliminomethyl)-2'-ethoxyphenyl-4-hexyloxybenzoate (4f)

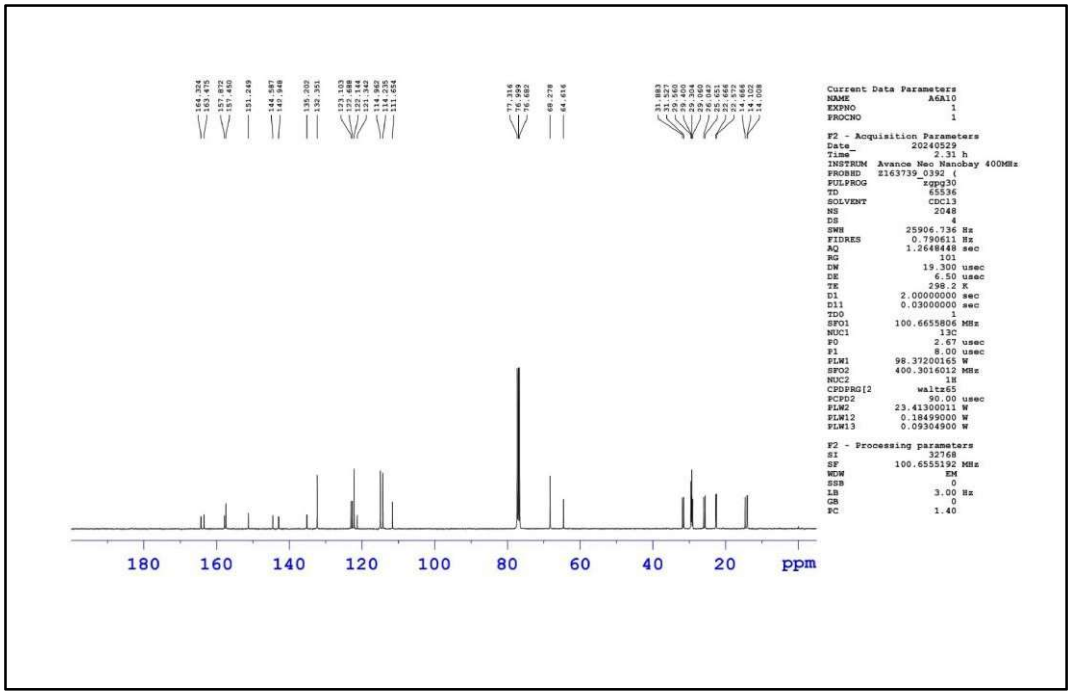

Figure 4.17: ^{13}C NMR spectra of 4'-(4''-decyloxyphenyliminomethyl)-2'-ethoxyphenyl-4-hexyloxybenzoate (4f)

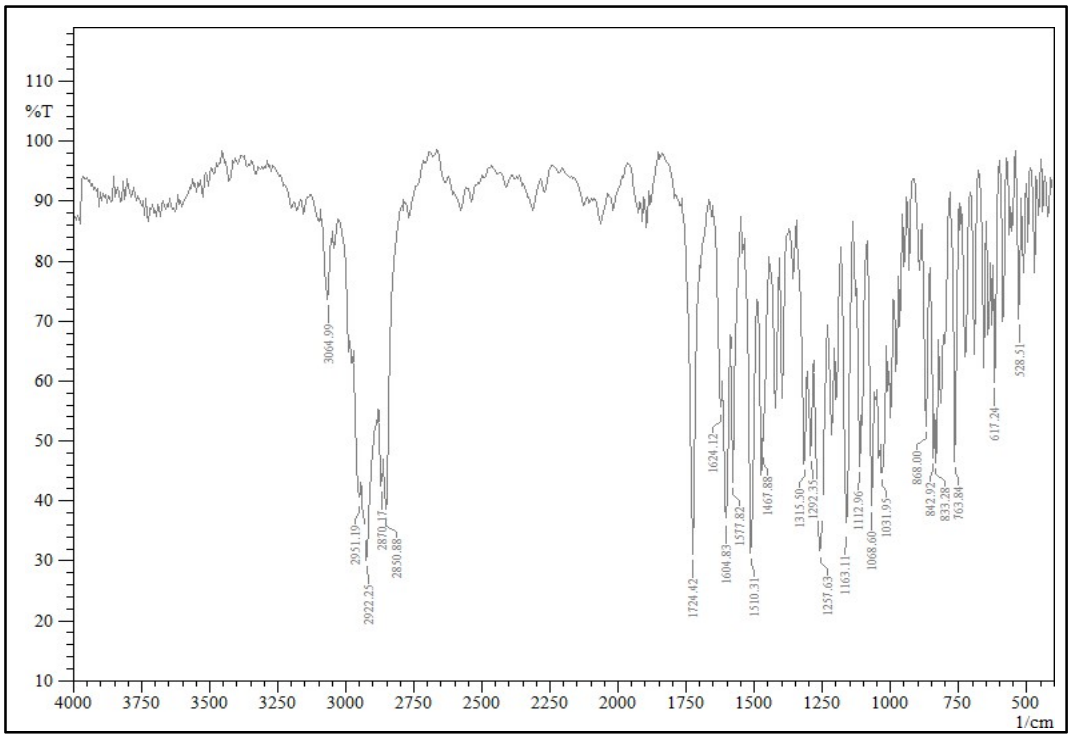

Figure 4.18: FT-IR spectra of 4'-(4"-decyloxyphenyliminomethyl)-2'-ethoxyphenyl-4-octyloxybenzoate (4h)

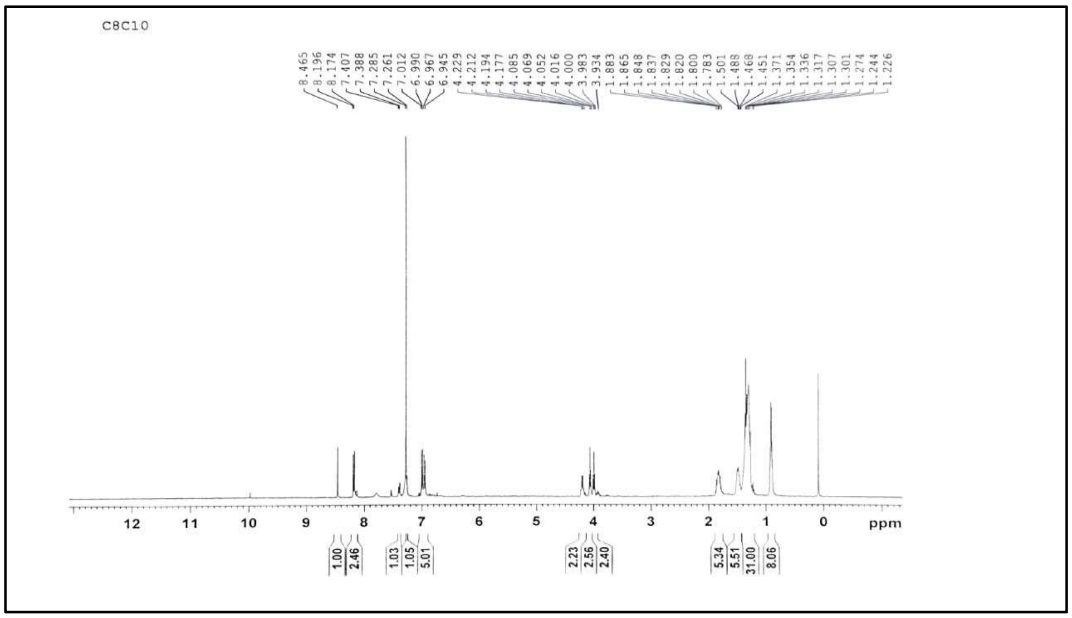

Figure 4.19: ^{1}H NMR spectra of 4'-(4"-decyloxyphenyliminomethyl)-2'-ethoxyphenyl-4-octyloxybenzoate (4h)

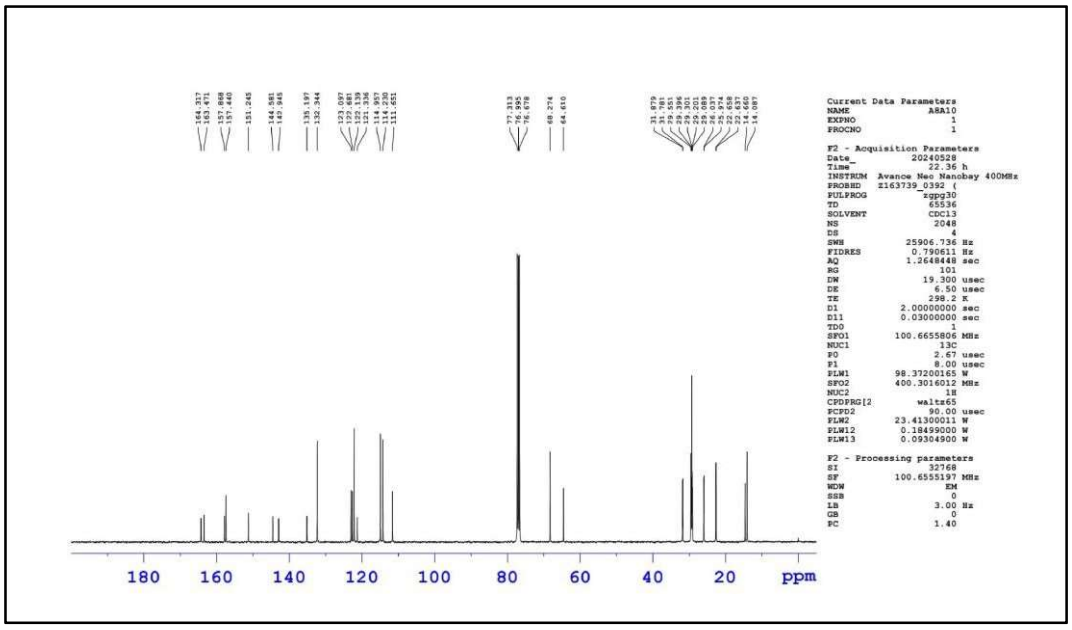

Figure 4.20: ^{13}C NMR spectra of 4'-(4''-decyloxyphenyliminomethyl)-2'-ethoxyphenyl-4-octyloxybenzoate (4h)

Table 4.1: Physical data of Series-I (4a-4m)

Compound code	n	Mol. Formula	% Yield	Elemental Analysis					
				Calculated (%)			Found (%)		
				C	H	N	C	H	N
4a	1	$C_{33}H_{41}NO_5$	76.30	74.55	7.77	2.63	76.51	7.10	2.50
4b	2	$C_{34}H_{43}NO_5$	75.11	74.83	7.94	2.57	73.79	7.51	2.48
4c	3	$C_{35}H_{45}NO_5$	77.58	75.10	8.10	2.50	75.26	8.89	2.78
4d	4	$C_{36}H_{47}NO_5$	78.15	75.36	8.26	2.44	75.60	8.50	2.50
4e	5	$C_{37}H_{49}NO_5$	76.10	75.61	8.40	2.38	76.10	8.18	2.54
4f	6	$C_{38}H_{51}NO_5$	77.48	75.84	8.54	2.33	75.18	8.34	2.10
4g	7	$C_{39}H_{53}NO_5$	77.50	76.06	8.67	2.27	76.15	8.50	2.45
4h	8	$C_{40}H_{55}NO_5$	75.06	76.27	8.80	2.22	76.50	8.81	2.67
4i	9	$C_{41}H_{57}NO_5$	78.51	76.48	8.92	2.18	77.10	8.98	2.40
4j	10	$C_{42}H_{59}NO_5$	79.73	76.67	9.04	2.13	76.10	9.12	2.67
4k	12	$C_{44}H_{63}NO_5$	80.51	77.04	9.26	2.04	77.50	9.56	2.45
4l	14	$C_{46}H_{67}NO_5$	79.33	77.38	9.46	1.96	77.50	9.10	1.89
4m	16	$C_{48}H_{71}NO_5$	76.14	77.69	9.64	1.89	77.10	9.51	1.80

To determine the mesomorphic character of the synthesized compounds, measurements of the transition temperatures and microscopic textures were taken during heating and cooling cycles. The compounds were then placed between two untreated glass slides and examined under an optical polarising microscope. To acquire more accurate transition temperatures, the observations were repeated and the rate of heating was adjusted to be low near the switch transition temperatures. The stability of every compound was observed following many heating and cooling cycles.

All synthesized compounds in Series I exhibit an enantiotropic nematic phase. With an optical polarising microscope, the nematic phase revealed a distinctive marble-like structure. It was discovered that there was a reasonable agreement between the phase transition temperatures obtained using a polarising optical microscope and the corresponding DSC thermograms.

4.3. Results and Discussion

All the synthesized compounds were prepared by condensation of 4-n-decyloxyaniline with 2'-ethoxy-4'-formylphenyl-4-alkoxybenzoate. All the compounds exhibit nematic phases. The synthetic route for the prepared series of mesogenic compounds is depicted in Scheme 4.1. Different enthalpy change values for Cr-N and N-I transition temperatures were noted in Table 4.3.

The synthesis and study of unusual liquid crystals have grown in importance and have attracted increasing attention recently due to advancements in liquid crystal science and technology [68-71]. Because of the -C=N- linkage in its basic structure and the lone pair electrons that the N atom possesses in its hybrid orbital, Schiff base liquid crystal has garnered significant attention in the rapidly advancing field of liquid crystal science [72]. The distinct end groups and center bridges significantly altered the stability and brightness of a single Schiff base liquid crystal [73, 74].

In addition to having rich LC morphology, LC compounds containing Schiff base could be employed to form LC composite films [75]. The composite film's selectivity to specific gases was enhanced by the atoms of nitrogen's affinity for oxygen. Effective manipulation and design of the LC molecular chain's sequence structure might alter the aggregation state structure and enthalpy of phase change of the LC molecules, resulting in LC molecules with various properties that could be used to create functional materials with various qualities.

A class of chemical compounds known as "Schiff bases" had imines or methylimine (-C=N-), and they were typically created when amines and activated carbonyl condensed. The domains of pharmacy, catalysis, analytical chemistry, corrosion, and photochromism were significantly impacted by Schiff base compounds and their metal complexes. Schiff base has shown good liquid crystal characteristics in the field of liquid crystal display. The imine bridge bond's strong polarity and stiffness caused a strong molecular contact, which made Schiff base compounds more likely to form liquid crystal phases. Schiff-based liquid crystal has drawn attention for a long time due to the rapid advancement of liquid crystal science.

Nematic mesophase molecules are oriented towards a specified direction known as the director, n, and have an orientational order in the nematic (N) phase but no positional order. The director orientation is represented by the unit vector(n). Despite their variation, the molecules' ends lack a preferred structure and can rotate in a nematic manner along their long axis. Molecules generating nematic crystalline mesophases in anisotropic forms typically feature stiff molecular backbones that characterize the long axis of the molecules. A higher probability of liquid crystallinity occurs when the molecules in the structures are composed of flat segments. Liquid crystalline compounds frequently contain groups that are easily polarizable and have strong dipole moments. The historical origin of the name "cholesteric" derived from their connection of cholesterol. The nematic mesophase, which has an orientational order, is comparable to the cholesteric mesophase. It is not the same as nematic mesophase, in which there is a weak propensity for surrounding molecules to align at a little angle. When chiral component molecules are present, it occurs. When chiral component molecules are present, there is a slight tendency.

That helical structure results from the process's unusual optical characteristics, such as selective reflection. When plane-polarized light interacts with this chiral macroscopic structure, the polarisation plane rotates in the direction of the helix.

The most popular tool for differentiating liquid crystal phases is the polarising optical microscope (POM), which displays the characteristic optical structure of a mesophase. Optical patterns are typically seen in thin layers of the sample, which have been chemically processed to produce either a homogenous or homeotropic arrangement of the molecules, between two glass plates. Depending on the strength of intra- and intermolecular interactions, liquid crystals form into different mesophase systems. They also exhibit the corresponding polarised optical microscopy (POM) textures for each phase, such as the smectic liquid crystal's fan-shaped focal

conic texture, the cholesteric liquid crystal's fingerprint texture, and the nematic liquid crystal's schlieren texture.

The terminal chains, lateral substituents, and core make up a mesogenic molecule. The terminal chains give stability to preserve the mesophase molecular alignment, whereas the core supplies the rigidity necessary for anisotropy. Usually, the aromatic ring at the center is connected linearly. The rings could be connected directly to one another or by the use of linking units such as -NH-CO-, -CH=CH-, -CH=N-, and -COO-. Although the terminal units are frequently polar substituents, the terminal chains are straight alkyl or alkoxy chains. Nematic or smectic mesophases are formed by the calamitic molecules, depending on the kind of substituents and their molecular arrangement.

To obtain azomethine compounds, Ha *et al.* (2011) synthesized 4-iodoaniline, condensed it with 4-hydroxybenzaldehyde, and refluxed the mixture in methanol for an hour [76]. Using ethanol and hexane for repeated recrystallization, all of the crude was refined until constant melting points were reached. Under a polarising optical microscope fitted with a hot stage and temperature regulator, liquid crystalline textures were distinguished.

Han *et al*. synthesized liquid crystals of azomethine with varying terminal chain lengths in 2012. It was observed that n-octanoyloxy exhibited smectic A and smectic B phases in n-dodecanoyloxy derivatives, whereas n-tetradecanoyloxy displayed monotropic B phases and enantiotropic smectic A phases in n-octadecanoyloxy derivatives.

The synthesis of 1,6-bis (formylphenoxy) hexane or 1,9-bis (formylphenoxy) nonane was reported by Kostromin *et al*. in 2012. This was achieved by polycondensing equimolar amounts of o-dianisidine with 1,6-bis (formylphenoxy) hexane or 1,9-bis (formylphenoxy) nonane in spacers of thermotropic polyazomethines, which have 6 and 9 methylene groups, respectively. In this work, following the initial heating scan that causes the Cr-LC phase change, compound exhibits an intense endothermal peak at 111 °C. This is followed by a lesser endothermal peak at 154 °C, which is caused by the LC-N transition phase. During the second heating scan, the glass transition can be quickly identified at 33 °C. However, during the first heating scan, the compound shows an intense endothermal peak at 33 °C that is caused by enthalpy relaxation in the solid phase. This is followed by a relatively modest endothermal peak at about 60 °C that is caused by the Cr-LC phase.

According to Naoum *et al*. (2015), the dipole moment of the mesogenic component of the molecule, which is dependent on the terminal polar group attached and the steric one, which varies depending on the substituent placement and length, is the primary factor determining the

stability and styles of mesophase growth [77]. A liquid crystalline compound's mesophase stability will decrease upon the addition of a substituent at the terminal position because of the steric influence of the terminal group, and its polarity anisotropy will either increase or decrease as a result of the polarising action of the substituent molecule [78].

Despite a large number of mesomorphic compounds being described, little is known about how variations in the molecular structure and composition affect the degree of anisotropy in the melt. It is evident by examining the formula of mesomorphic compounds that the main length of each molecule unites them all. The rod-like structure of the molecules supports Friedel's linear molecular arrangement for the smectic and nematic phases. Any dipoles inside the molecules will increase the strong inclination for such molecules to lie with their long axes parallel. It has been discovered that mesomorphism only occurs in molecules wider than benzene.

Thermotropic liquid crystals are very important for technology. There have been many mesogenic compounds reported that exhibit nematic or other mesophases and feature the naphthalene moiety as its core system. Dave and colleagues investigated a range of liquid crystalline compounds with naphthalene moiety that exhibited smectic, nematic, and cholesteric mesomorphism; Vora and Prajapati also reported the mesogenic homologous series of Schiff's base-esters with naphthalene moiety and investigated the impact of lateral thiol and methoxy substituent on mesomorphism. Tetra-acylated 1,4,5,8-tetrahydroxynaphthalene derivatives were synthesized by Malthete *et al*. A sizable number of research studies on naphthalene liquid crystal cores have been published in the literature throughout the past ten years.

Three comparable series of symmetric, banana-shaped, liquid crystalline molecules with bis naphthyl units were synthesized and characterized by Yang and Lin. Two fused-ring structures, 6-n-decyloxy-2-naphthoic acid, and 6-dodecyloxyisoquinoline, were synthesized by Lin *et al*. [29] and utilized as a proton donor and acceptor moieties to build many basic mesogenic supramolecules. The remaining complementary hydrogen-bonded (H-bonded) moieties include pyridines with varying alkyl chain lengths joined by ether and ester bonds, benzoic acids, and thiophenecarboxylic acids.

4.3.1 Texture Analysis of Series-I

In Series-I, the homologue from **(4a–4m)**, first showed a nematic phase with a characteristic threaded marble-like texture when melted, but it later transformed into an isotropic liquid upon further heating. The sample exhibits nematogenic textures upon cooling, which, upon

additional cooling at a specific temperature, transform into a crystalline substance. After heating compound **4d** to 130.1 °C, threaded marble-like droplets nematic phase textures were observed. (Figure 4.21). Compound **4d** exhibits the Cr-N transition (Figure 4.22) at 130.1 °C. At 134.8 °C, a little curve (Figure 4.22) that represents the N-Iso transition (compound **4d**) was seen. As the sample cooled, two tiny curves representing the Iso-N and N-Cr transitions with negligible enthalpy changes were seen at two distinct temperatures (131.5 °C and 45.1 °C). Similarly, the compounds (**4a–4m**) show textures of the nematic phases upon heating; and on further heating forms a typical threaded marble-like texture of the nematic phase. Nematic textures were seen when it cooled from the isotropic melt, and then the characteristic textures of nematic phases were seen with further cooling. Thus, all of the suggested compounds were shown to be enantiotropic when examined with a polarising optical microscope.

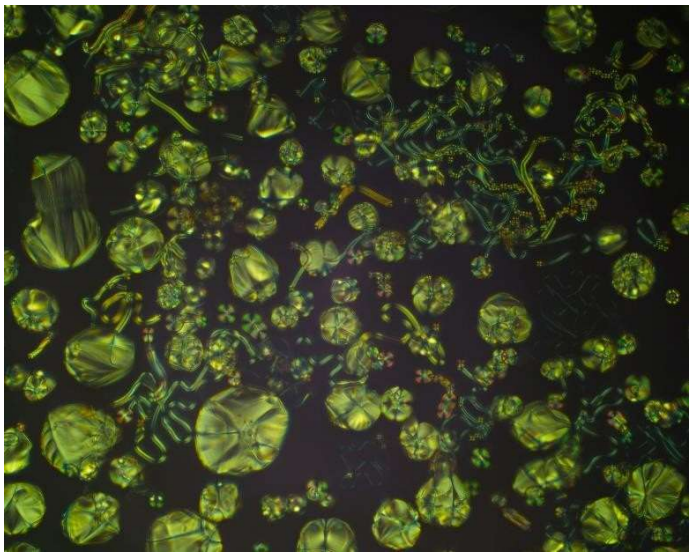

Figure 4.21: Microscopic texture of threaded nematic marble like droplets of compound **4d** at 130.1 °C on heating.

4.3.2 Thermal properties of Series-I

The DSC analysis yields the enthalpy change (ΔH). Table 4.3 lists the transition temperature (°C) along with the transition enthalpy change (kJ mol^{-1}) values for compounds **4a–4m** after heating and cooling. The enantiotropic mesophase was confirmed by compounds **(4a–4m)** showing two peaks corresponding to crystal-nematic (Cr–N) and nematic-isotropic (N-Iso) with differing transition enthalpy change values. All of the compounds stability was noted after several cycles of heating and cooling. A nematic to isotropic transition of compound **4d** is observed at 134.8 °C, with one peak observed on cooling at 131.5 °C with an enthalpy change

of 0.32 kJ/mol attributed to the Iso-N transition. The endothermic peak was observed at 130.1 °C as an enthalpy change of 9.90 kJ/mol, which is attributed to the Cr-N transition (Figure 4.22). This confirms compound **4d** as a pure nematogen.

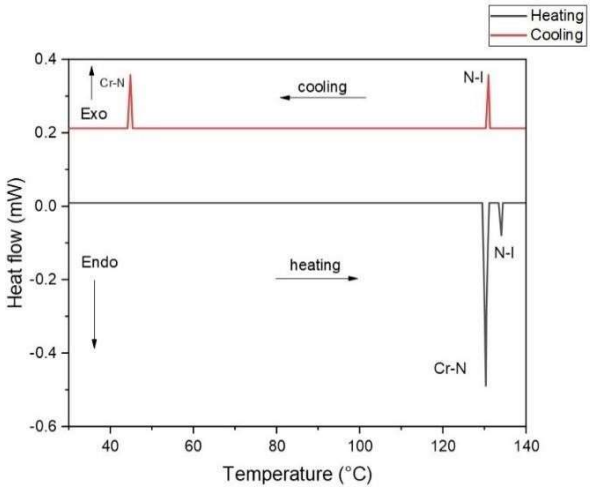

Figure 4.22: DSC of compound **4d**

Figure 4.23 shows that after heating compound **4e** to 97.1 °C, an endotherm curve with a corresponding phase transition change in enthalpy of 9.80 kJ/mol was observed, indicating the Crystal-Nematic transition. After heating the compound further, another peak with an enthalpy of 0.40 kJ/mol was observed at 126.3 °C, a very small curve showing the N-Iso transition was observed. With a change in enthalpy of 0.35 and 8.90 kJ/mol upon cooling, the exothermic curve at 100.1 °C and 46.1 °C corresponds to the Iso-N to N-Cr transition. The aforementioned information evaluates the chemical **4e**'s enantiotropic behaviour.

In heating and cooling cycles, all of the compounds (**4a–4m**) display enantiotropic mesophases at varying phase transition enthalpy change values. The phase transition enthalpy change values, which were assigned in Table 4.3, are initially reasonably predicted during the Cr-N/N-Cr transition. Conversely, it is found that the enthalpy change values for N-Iso/Cr-N are lower than anticipated.

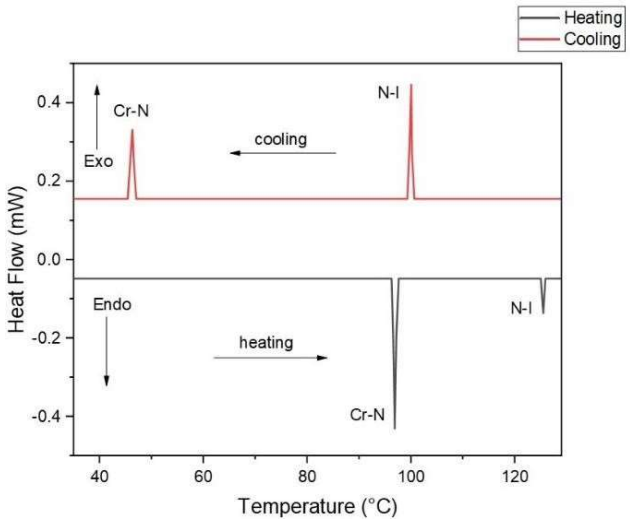

Figure 4.23: DSC of compound **4e**

Table 4.2: Transition temperatures of compounds (4a-4m) taken on polarizing optical microscope [Series-I]

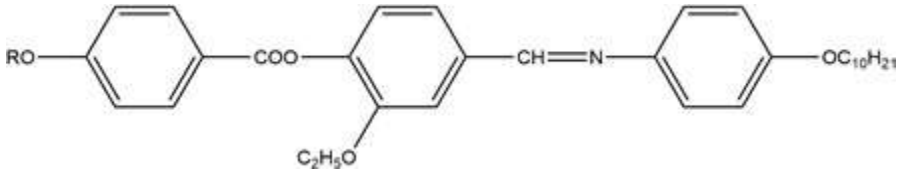

Sr. No.	R = *n*-alkyl group	Transition temperatures (°C)				
		Cr		N		I
1	Methyl	•	111.1	•	127.7	•
2	Ethyl	•	142.5	•	145.1	•
3	Propyl	•	132.1	•	135.0	•
4	Butyl	•	130.1	•	134.8	•
5	Pentyl	•	97.1	•	126.3	•
6	Hexyl	•	85.8	•	132.5	•
7	Heptyl	•	88.1	•	125.8	•
8	Octyl	•	92.1	•	116.5	•
9	Nonyl	•	85.5	•	122.7	•
10	Decyl	•	84.1	•	120.1	•
11	Dodecyl	•	82.5	•	123.3	•
12	Tetradecyl	•	84.1	•	118.2	•
13	Hexadecyl	•	87.1	•	120.1	•

Table 4.3: Transition temperatures (°C) along with enthalpy change (ΔH) (kJ mol-1) and for compounds 4a-4ma upon heating and cooling [Recorded in Differential Scanning Calorimetry]

Compound code	n-alkyl group	Transition temperatures(°C)		$\Delta S_{CrN}/R$ Heating	$\Delta S_{NI}/R$ Heating	$\Delta S_{IN}/R$ Cooling	$\Delta S_{NCr}/R$ Cooling
		Heating Temp.°C[ΔH kJ mol^{-1}]	Cooling Temp.°C[ΔH kJ mol^{-1}]				
4a	1	Cr 111.5[11.90] N 127.7[0.45] I	I 115.1[0.39] N 60.3[11.10] Cr	20.94	0.77	0.68	29.72
4b	2	Cr 142.5[10.10] N 145.1[0.88] I	I 143.1[0.65] N 69.3[9.56] Cr	17.93	1.53	1.16	25.69
4c	3	Cr 132.1[8.80] N 135.1[0.90] I	I 133.4[0.82] N 40.2[8.25] Cr	16.05	1.59	1.50	21.57
4d	4	Cr 130.1[9.90] N 134.8[0.35] I	I 131.5[0.32] N 45.1[9.10] Cr	18.22	0.62	0.59	24.99
4e	5	Cr 97.1[9.80] N 126.3[0.40] I	I 100.1[0.35] N 46.1[8.90] Cr	17.87	0.71	0.64	23.83
4f	6	Cr 85.8[8.85] N 132.5[0.10] I	I 90.1[0.08] N 50.4[8.10] Cr	16.03	0.17	0.14	21.40
4g	7	Cr 88.1[6.60] N 125.8[0.20] I	I 91.1[0.15] N 52.3[6.10] Cr	12.19	0.35	0.28	16.29
4h	8	Cr 92.1[7.80] N 116.5[0.11] I	I 95.1[0.09] N 60.1[7.21] Cr	14.46	0.19	0.16	17.88
4i	9	Cr 85.5[8.81] N 122.7[0.06] I	I 118.7[0.05] N 67.2[8.10] Cr	16.42	0.10	0.09	20.44
4j	10	Cr 84.1[8.21] N 120.1[0.10] I	I 116.1[0.08] N 65.5[7.65] Cr	15.38	0.18	0.15	19.45
4k	12	Cr 82.5[7.95] N 123.3[0.25] I	I 110.2[0.20] N 54.9[7.10] Cr	14.92	0.46	0.37	17.96
4l	14	Cr 84.1[6.50] N 118.2[0.10] I	I 100.1[0.07] N 58.5[6.01] Cr	12.27	0.18	0.13	15.07
4m	16	Cr 84.1[7.50] N 118.2[0.30] I	I 100.1[0.25] N 58.5[6.91] Cr	14.14	0.55	0.47	17.30

Cr-crystalline solid, N-nematic mesophase, I-isotropic liquid

[a]Phase transition temperatures were noted by Differential Scanning Calorimetry studies: peak temperatures in the DSC thermograms obtained during the first heating and cooling cycles (scanning rate = 5 °C min^{-1}).

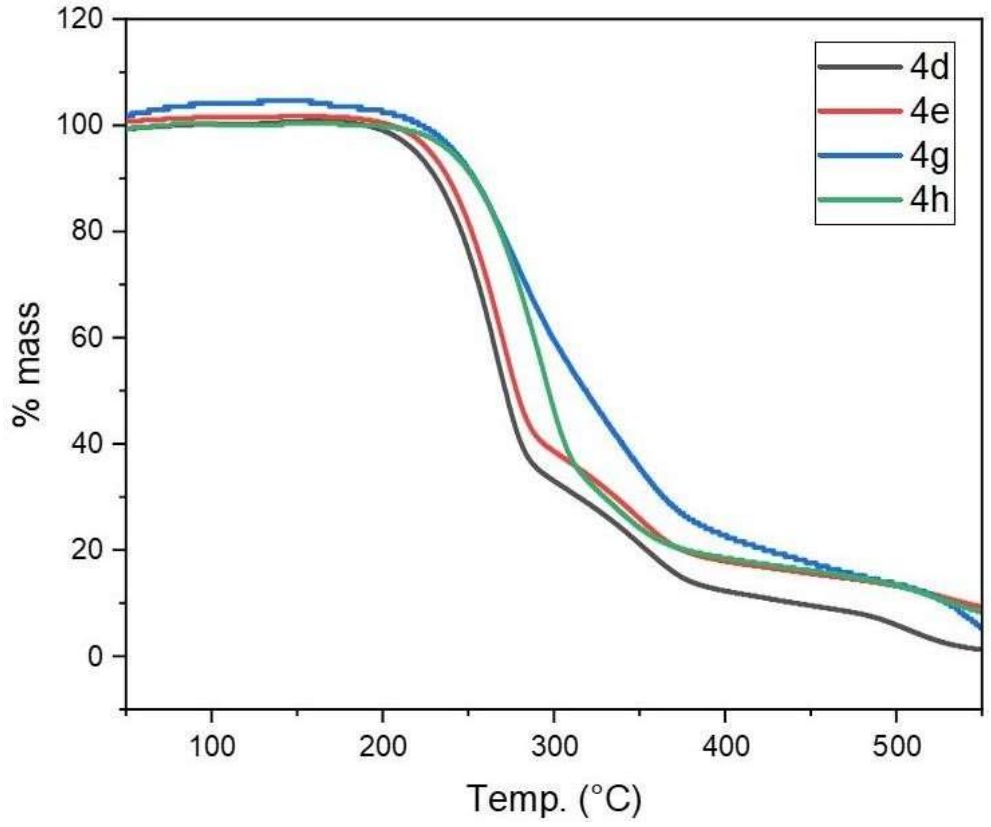

Figure 4.24: Representative TGA thermogram of compounds **4d**, **4e**, **4g**, **and 4h** was recorded under nitrogen atmosphere.

Compounds 4d, 4e, 4g, and 4h, performed TGA measurements in a nitrogen environment at temperatures between 50 and 550 °C. In Figure 4.24, the compounds TG curves are displayed. The thermal stability of the obtained compounds was attributed to the observation that all of the unsymmetrical derivatives of series-I are thermally stable up to 180 °C.

Table 4.4: TGA thermograms decomposition for compounds 4d, 4e, 4g and 4h

Compound code	IDT (°C)	50% DT (°C)	FDT (°C)
4d	176	260	550
4e	178	268	552
4g	175	288	555
4h	180	290	560

The initial degradation temperature (IDT), 50% decomposition temperature, and the final decomposition temperature (FDT) for each respective derivative are provided in Table 4.4. In particular, the compounds exhibit LC properties before undergoing thermal decomposition. Compound 4h had the greatest initial thermal decomposition temperature, which was 180 °C,

whereas compound 4g displayed the lowest IDT, which was 175 °C. The observations presented here suggest that there is a lower probability of thermal decomposition occurring within this temperature range, as shown in Figure 4.4 respectively. In addition, the decomposition process was completed within the range of 550 to 560°C, and the 50% decomposition of all of the derivatives that were investigated took place within the temperature range of 260 to 290 °C.

4.3.3 Structure-mesomorphic relationship

From the transition temperatures (°C) and transition enthalpy change values, it was observed that (**4a-4m**) derivatives exhibit a pure nematic phase only. Figure 4.25 represents the mesogenic behaviour as a function of the number of carbon atoms in the alkoxy chain for the transition temperature of the novel synthesized compounds. In the crystal-mesophase transition, as we ascend the series the rising trend was observed till the n-ethyl derivative (**4b**) followed by the decreasing trend till the n-hexyl derivative (**4f**), with the increase in methylene unit, the increasing trend was observed till the compound **4h,** and the falling tendency was observed till n-dodecyl derivative (**4k**) followed by the rising curve till compound **4m**. In the N-Iso transition, the alternate rising-falling tendency was observed till the n-hexyl derivative (**4f**), after that characteristic decrease in the trend was observed till compound **4h**, followed by a rising-falling trend in transition temperature till compound **4m**.

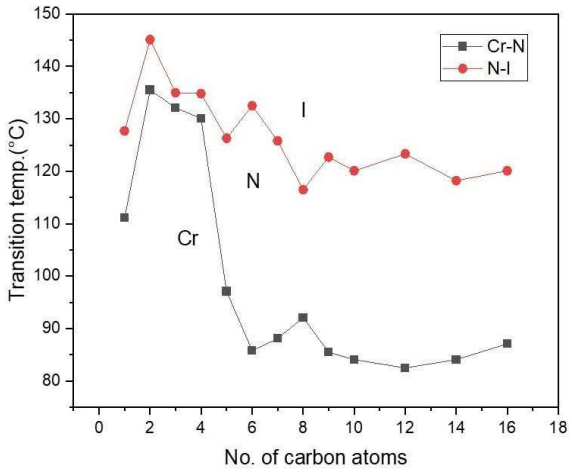

Figure 4.25: Variation of transition temperatures with a number of carbon atoms in the alkoxy chain of the mesogenic compounds of Series-I

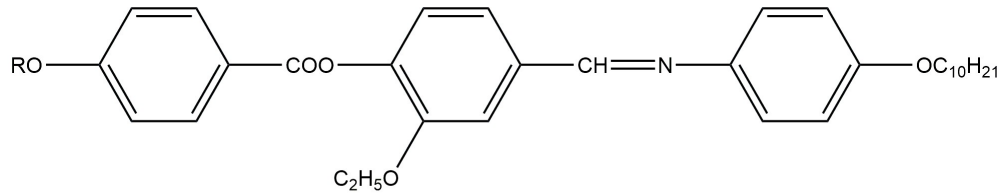

Series-I

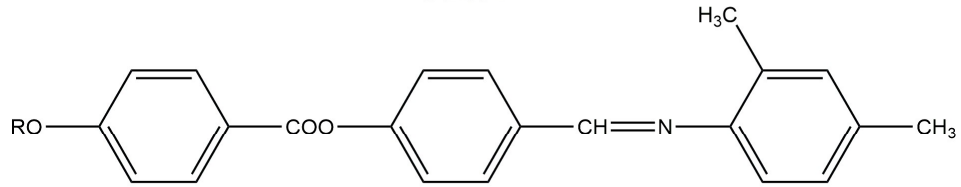

Series A

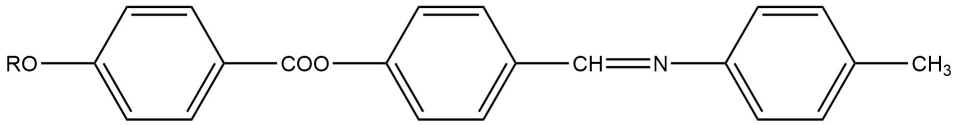

Series B

The average thermal stabilities of different mesogenic homologous series are compared and recorded in Table 4.5.

Table 4.5: Average thermal stabilities (°C) of Series-I, A and B compounds.

Series	I	A	B
N-Iso	126.7 (C_1-C_{10},C_{12},C_{14},C_{16})	177.5 (C_1-C_{10},C_{12},C_{14},C_{16})	224.5 (C_1-C_{10},C_{12},C_{14},C_{16})
Cr-N	107.1 (C_1-C_9)	99.6 (C_1-C_9)	102.1 (C_1-C_9)

An unsymmetrical series of compounds (**4a-4m)** contains 4-n-decyloxyaniline linked with 2'-ethoxy-4'-formylphenyl-4-alkoxybenzoate forming an imine linkage. According to Grey *et al.* [81], the decrease in nematic thermal stability is unrelated to the cis or trans geometry that the molecule adopts. Therefore, it is possible to understand the average decline in nematic thermal stability in the reported series. In comparison to Series I and Series B, the cis geometry of Series A shows an increase in molecular breadth. Hence, there will be a decrease in lateral

intermolecular attraction and, as a result, nematic thermal stability. Hence, the decrease in lateral intermolecular attraction and consequently the decrease in nematic thermal stability is observed in series A as compared to Series I and B. The molecular arrangement in Series A causes the molecule less coplanar (due to the steric effect between the methyl substituent and the hydrogen of the –N=CH- unit) compared to Series I and Series B. Again the lateral intermolecular attractions are reduced and a decrease in thermal stability of nematic phase is observed in Series A.

4.4. References

[1] Brown GH. Structure, properties and some applications of liquid crystals. J. Opt. Soc. Am. 1973; **63**(12):1505-1514.

[2] Zhao Y, et al. Orientation and anchoring effects in stretched polymer dispersed nematic liquid crystals. 2000; **27**(9):1183-1187.

[3] Akkurt N, et al. Synthesis and liquid crystalline properties of new triazine-based conjugated macromolecules with chiral side groups. Turk. J. Chem. 2020; **44**(3):726-735.

[4] Cuerva C, et al. Columnar discotic Pt(II) metallomesogens as luminescence multifunctional materials with chemo and thermosensor abilities. J.Mater.Chem.C. 2014; **2**(43):9167-9181.

[5] Cheng H, et al. Polycanter bent shaped liquid crystals with columnar and cubic phases: Synthesis multiresponsive organogels and chemosensors. J.Mol.Liq. 2018; **249**(1):723-731.

[6] Zhang M, et al. Nematic liquid crystals materials as a morphology regulator for ternary small molecule solar cells with power conversion efficiency exceeding 10%. J. Mater. Chem. A. 2017; **5**(7):3589-3598.

[7] Rathod SL, et al. Blue light-emitting quinoline armed Thiacalix [4] arene 3D-scaffold. A systematic platform to construct fluorescent liquid crystals with bio-imaging applications. J. Mol. Str. 2022; **1270**:133830.

[8] Madiahlagan E, et al. Synthesis, liquid crystalline properties and photo switching properties of coumarin-azo bearing aliphatic chains: Applications in optical storage devices. J.Mol.Liq. 2019; **292**:111328.

[9] Hird M. Ferroelectricity in liquid crystals-materials, properties and applications. Liq. Cryst. 2011; **38**(11–12):1467-1493.

[10] Teucher I, Paleos CM, and Labes MM. Properties of Structurally Stabilized Anil Type Nematic Liquid Crystals. Mol. Cryst. Liq. Cryst. 1970; **11**(2):187-189.

[11] Sharma VS, and Patel RB. Effect of Alkyl chain in the terminal ester group on mesomorphic properties of new rod-like homologous series: Synthesis and characterization Mol. Cryst. Liq. Cryst. 2017; **643**(1):62-75.

[12] Kim Y, et al. The effect of surface polarity of glass on liquid crystal alignment. Liq. Cryst. 2018; **45**(5):757-764.

[13] Ranjkesh A, et al. New linear solvation energy relationships for empirical solvent scales using the Kamlet-Abboud –Taft parameter sets in nematic liquid crystals. RSC Adv. 2018; **8** (40):22835-22845.

[14] Haase W, and Wedel H. The Applications of Nematic Liquid Crystals as Anisotropic Solvents in the Optical Absorption Spectroscopy for the Determination of the Polarization of Electronic Transitions of Organic Molecules and Cu(II) complexes. Mol. Cryst. Liq. Cryst. 1977; **38**(1):61-76.

[15] Zhu X, et al. Some new azobenzene liquid crystals involving chalcone and ester linkages. RSC Adv. 2007; **7**(73):46344-46353.

[16] Niori T, Sekine F, Watanabe J, Furakawa T, Takezoe H. J. Distinct ferroelectric smectic liquid crystals consisting of banana shaped achiral molecules. Mater. Chem. 1996; **6**(7):1231–1233.

[17] Lee J, and Lee SD. Ferroelectric Liquid Crystalline Ordering of Rigid Rods with Dipolar Interactions. 1994; **254**(1):395-403.

[18] Matsunaga Y. Yuri T. Mesomorphic behaviour of N,N'-Bis[4-(4-alkoxybenzoyloxy)benzylidene-3-3'-diaminodiphenylsulphones. Mol. Cryst. Liq. Cryst. 1993; **237**(1):145–150.

[19] Akutagawa T, Matsunaga Y, Yashahura K. Mesomorphic behaviour of 1,3-phenylene bis[4-(4-alkoxyphenyliminomethyl)benzoates] and related compounds. Liq. Cryst. 1994; **17**(5):659–666.

[20] Bezborodov VS and Petrov VF. Lateral substitution in nematic systems. Liq. Crystals. 1997; **23**(6):771-788.

[21] Bezborodov VS, et al. The synthesis and properties of some mesomorphic cyclohexene properties. Liq. Crystals. 1997; **23**(1):69-75.

[22] Petrov VF, et al. The trans 1,4-cyclohexylene group as a structural fragments in liquid crystals. Liq. Crystals. 1999; **26**(8):1141-1162.

[23] Hird M. Toyne KJ, Gray GW; McDonnell DG; Sage IC. The relationship between molecular structure and mesomorphic properties of 2,2' and 3,2'-difluoroterphenyls Liq. Cryst. 1995; **18**(1):1–11.

[24] Sugiura, H, Sakurai Y, Masuda Y, Takeda H, Kusabayashi S, Takenaka S. The substituent effect on mesomorphic properties of 4-octyloxyphenyl 4-(nitrobenzoyloxy)benzoates. Liq. Cryst. 1991; **9**(3):441–450.

[25] Masuda Y, Sakurai Y, Sugiura H, Miyake S, Takenaka S, Kusabayashi S. The effect of a lateral substituents on the mesomorphic properties of 4-cyanophenyl 4-(4alkyloxybenzoyloxy)benzoates. Liq. Cryst. 1991; **10**(5):623–634.

[26] Dabrowski R, Bezborodov VS, Lapanik VJ, Dziaduszek J, Czuprinski K. Mesomorphic properties of phenyl 4-(5-alkyl-1,3,2-dioxaborin-2-yl) benzoates Influence of terminal and lateral substituents. Liq. Cryst. 1995; **18**(2):213–218.

[27] Petrov VF. Halogenation in achiral liquid crystals: terminal and linking substitutions. 2001; **28**(3):387-410.

[28] Thaker BT, Kanojiya JB. Mesomorphic properties of liquid crystalline compounds with biphenyl moiety containing azo-ester, azo-cinnamate linkages and different terminal group. Liq Cryst. 2011; **38**(8):1035–1055.

[29] Chauhan ML, Pandya RN, Doshi AV. Synthesis and mesomorphism of novel liquid crystalline: p-(p ′-n-alkoxy benzoyloxy) methyl cinnamates. Mol Cryst Liq Cryst. 2011; **548**(1):228–234.

[30] Selvarasu C, Kannan P. Alkyloxy azo-cinnamate ester based thermotropic liquid crystals and their photophysical investigations. Mol Cryst Liq Cryst. 2017; **648**(1):77–87.

[31] Jain BB, Sharma VS, Chauhan HN, et al. Mesomorphism of azo-esters and chalcone-esters. Mol Cryst Liq Cryst. 2016; **630**(1):102–111.

[32] Karim MR, Sheikh MRK, Yahya R, et al. The effect of terminal substituents on crystal structure, mesophase behaviour and optical property of azo-ester linked materials. Liq Cryst. 2016; **43**(12):1862–1874.

[33] Jadeja UH, Patel RB The effect of molecular rigidity and flexibility on the mesomorphism of azoesters. Mol Cryst Liq Crystals. 2016; **637**(1):28–36.

[34] Jain BB, Jadeja UH, Patel RB. Molecular flexibility operated mesomorphism by end groups in azoester series. Mol Cryst Liq Cryt. 2017; **652**(1):1–9.

[35] Thaker BT, Kanojiya JB, Tandel RS. Effects of different terminal substituents on the mesomorphic behavior of some azo-schiff base and azo-ester-based liquid crystals. Mol Cryst Liq Cryst. 2010; **528**(1):120–137.

[36] Naoum MM, Mohammady SZ, Ahmed HA. Lateral protrusion and mesophase behavior in pure and mixed states of model compounds of type 4-(4′-substituted phenylazo)-2-(or 3-methylphenyl-4”-alkoxy benzoates. Liq Cryst. 2010; **37**(10):1245–1257.

[37] Naoum MM, et al. Effect of exchange of terminal substituents on the mesophase behaviour of some azo/ester compounds. Liq. Cryst. 2014; **41**(11):1559-1568.

[38] Naoum MM, Metwally NH, Abd Eltawab MM. et al. Ahmed. Polarity and steric effect of the lateral substituent on the mesophase behaviour of some newly prepared liquid crystals. Liq Cryt. 2015; **42**(10):1351–1369.

[39] Sharma VS, Jadeja UH, Patel RB. Study of the molecular structure of liquid crystal properties regarding thermotropic azoester derivatives. Mol cryst Liq Cryst. 2017; **643**(1):28–39.

[40] Saad GR, Ahmed NHS. Fahmi AA and Naoum MM. Effect of orientation of lateral methyl substituent on the thermal behaviour of the mesophase in binary systems of 4-substituted phenyl 4′-(4”-alkoxyphenylazo) benzoates. Liq Cryt. 2018; **45**(8):1177–1185.

[41] Ahmed NHS, Saad GR and Naoum MM. Effect of position of the lateral fluoro substituent on the mesophase behaviour of aryl 4-alkoxyphenylazo benzoates in pure and binary mixtures. Liq Cryt. 2018; **45**(10):1487–1497.

[42] Mahmoud NE, Saad GR, Fahmi AA, et al. Effect of including extra phenylazo moiety on the mesophase behaviour of three-ring azo/ester molecules. Liq Cryst. 2018; **45**(11):1711–1722.

[43] Naoum MM, Ahmed HA, Fahmi AA. Liquid crystalline behavior of model compounds di-laterally substituted with different polar groups. Liq Cryst. 2011; **38**(1):511–5199.

[44] Thaker BT, Dhimmar YT, Patel BS, et al. Studies of calamitic liquid crystalline compounds involving esterazo central linkages with a biphenyl moiety. Mol Cryt Liq Cryst. 2011; **548**(1):172–191.

[45] Dixit S, Vora RA. Novel azoester compounds with a lateral methyl substituent. Mol Cryst Liq Cryst. 2014; **592**(1):133–140.

[46] Ahmed HA, Saad GR. Mesophase behaviour of laterally di-fluoro-substituted four-ring compounds. Liq Cryst. 2015; **42**(12):1765–1772.

[47] Patel DH, Prajapati HR, Doshi AV. Mesomorphism dependence on lateral substitution of functional groups and their position in series: 4(4′-n-alkoxy benzoyloxy)- 3-chloro phenyl azo-2″-methoxy benzenes. Mol Cryt Liq Cryst, 2016; **624**(1):151-158.

[48] Naoum MM, Fahmi AA, Ahmed NHS, et al. The effect of inversion of the ester group on the mesophase behavior of some azo/ester compounds. Liq Cryst. 2015; **42**(9):1298–1308.

[49] Naoum MM, Fahmi AA, Ahmed NHS, et al. The effect of lateral methyl substitution on the mesophase behavior of aryl 4-alkoxyphenylazo benzoates. Liq Cryst. 2015; **42**(11):1627–1637.

[50] Saha SK, Paul MK, Chandran A, et al. Low-temperature nematic phase in asymmetrical 1,3,4-oxadiazole bent-core liquid crystals possessing lateral methoxy group. Liq Cryst. 2017; **44**(11):1739–1750.

[51] Perju E, Cozan V, Timpu D, et al. The influence of methoxy side groups and halogen nature on the mesomorphic and optical properties of symmetrical azomethines. Liq Cryst. 2017; **44**(5):798–808.

[52] Naoum MM, Fahmi AA, Saad GR, et al. Polarity and steric effect of di-lateral substitution on the mesophase behaviour of some azo/ester compounds. Liq Cryst. 2017; **44**(11):1664–1677.

[53] Duan LY, Shi DQ, Chen P, et al. Preparation and properties of laterally multifluorinated benzoxazole-based nematic mesogens. Liq Cryst. 2017; **44**(11):1686–1694.

[54] Jadeja UH, Sharma VS, Jain BB & Patel RB. Dependence on LC state on molecular flexibility. Liq. Cryst. 2016; **630**(1):144-153.

[55] Goodby JW, Mandle RJ, Davis EJ, et al. What makes a liquid crystal? The effect of free volume on soft matter. Liq Cryst. 2015; **42**(5-6):593–622.

[56] Goodby JW. Free volume, molecular grains, self-organization, and anisotropic entropy: machining materials. Liq Cryst. 2017; **44**(12–13):1755–1763.

[57] Luo CC, Jia YG, Sun BF, Meng FB. The effect of chain length in terminal groups on the mesomorphic behavior of novel (−)-menthol-based chiral liquid crystal compounds with a blue phase. New J. Chem. 2017, **41**(1):3677–3686.

[58] Cheng Z, Li K, Wang F, Wu X, Chen X, Xiao J, Zhang H, Cao H, Yang H. Influence of linkage and terminal group on the liquid crystalline and helical twisting behaviour of cholesteryl esters. Liq. Cryst. 2011, **38**(7):803–812.

[59] Hagar M, Ahmed H, Aouad M. Mesomorphic and DFT diversity of Schiff base derivatives bearing protruded methoxy groups. Liq. Cryst. 2020; **47**(14-15):2222–2233.

[60] Hagar M, Ahmed H, Saad G. New calamitic thermotropic liquid crystals of 2-hydroxypyridine ester mesogenic core: Mesophase behaviour and DFT calculations. Liq. Cryst. 2020; **47**(1):114–124.

[61] Rodrigues LD, Sunil D, Chaithra D, Bhagavath P. 1, 2, 3/1, 2, 4-Triazole containing liquid crystalline materials: An up-to-date review of their synthetic design and mesomorphic behavior. J. Mol. Liq. 2020; **297**(1):111909.

[62] Olate FA, Parra ML, Vergara JM, Barbera J, Dahrouch M. Star-shaped molecules as functional materials based on 1, 3, 5-benzenetriesters with pendant 1, 3, 4-thiadiazole groups: Liquid crystals, optical, solvatofluorochromic and electrochemical properties. Liq. Cryst. 2017; **44**(7):1173–1184.

[63] Sharma VS, Shah AP, Sharma AS. A new class of supramolecular liquid crystals derived from azo calix [4] arene functionalized 1, 3, 4-thiadiazole derivatives. New J. Chem. 2019; **43**(8):3556–3564.

[64] Kelker H, Scheurle B. A liquid-crystalline (nematic) phase with a particularly low solidification point. Angew. Chem. Int. Ed. Engl. 1969, **8**(11), 884–885.

[65] Hagar M, Ahmed H, El-Sayed T, Alnoman R. Mesophase behavior and DFT conformational analysis of new symmetrical diester chalcone liquid crystals. J. Mol. Liq. 2019; **285**:96–105.

[66] Ahmed HA, Hagar M, El-Sayed TH. Alnoman RB. Schiff base/ester liquid crystals with different lateral substituents: Mesophase behaviour and DFT calculations. Liq. Cryst. 2019; **46**(7):1–11.

[67] Hird M, Toyne KJ, Gray GW, Day SE, & McDonnell DG. The synthesis and high optical birefringence of nematogens incorporating 2,6-disubstituted naphthalenes and terminal cyano-substituent, Liq.Cryst. 1993; **15**(2):123-150.

[68] Sidir YG. The solvatochromism, electronic structure, electric dipole moments and DFT calculations of benzoic acid liquid crystals. Liq Cryst. 2020; **47**(10):1435–1451.

[69] Imrie CT, Henderson PA, Yeap GY. Liquid crystal oligomers: going beyond dimers. Liq Cryst. 2009; **36**(6–7):755–777.

[70] Imrie CT, Lu ZB, Picken SJ, et al. Oligomeric rod-disc nematic liquid crystals. Chem Commun. 2007; **12**(12):1245–1247.

[71] Attard GS, Date RW, Imrie CT, et al. Non-symmetric dimeric liquid crystals -the preparation and properties of the alpha-(4-cyanobiphenyl-4′-yloxy)-omega-(4-nalkylanilinebenzylidene-4′-oxy) alkanes. Liq Cryst. 2006; **36**(11–12):1455–1485.

[72] Smith JA, DiStasio RA, Hannah NA, et al. SF 5-terminated fluorinated Schiff base liquid crystals. J Phys Chem B. 2004; **108**(52):19940–19948.

[73] Paterson DA, Crawford CA, Pociecha D, et al. The role of a terminal chain in promoting the twist-bend nematic phase: the synthesis and characterisation of the 1-(4-cyanobiphenyl-4′-yl)-6-(4-alkyloxyanilinebenzylidene-4′-oxy) hexanes. Liq Cryst. 2018; **45**(13–15): 2341–2351.

[74] Yeap GY, Hng TC, Yeap SY, et al. Why do nonsymmetric dimers intercalate? The synthesis and characterisation of the-(4-benzylidene-substituted-aniline -4′-Oxy)- (2-methylbutyl-4′-(4′’-phenyl)benzoateoxy) alkanes. Liq Cryst. 2009; **36**(12):1431–1441.

[75] Meier H, Lehmann M, Holst HC. Star-shaped conjugated compounds forming nematic discotic systems. Tetrahedron. 2004; **60**(32):6881–6888.

[76] Ha ST, Lee TL, Yeap GY, Ito MM, Saito A, Watanabe M. Mesomorphic Behavior of New Azomethine Liquid Crystals Having Terminal Iodo Group. Chin. Chem. Lett. 2011; **22**(3): 260–263.

[77] Naoum MM, Metwally NH, Abd eltawab MM, Ahmed HA. Polarity and Steric Effect of the Lateral Substituent on the Mesophase Behaviour of Some Newly Prepared Liquid Crystals. Liq. Cryst. 2015; **42**(10):1351–1369.

[78] Hagar M, Ahmed H, Hussien T, Alnoman R. Mesophase Behavior and DFT Conformational Analysis of New Symmetrical Diester Chalcone Liquid Crystals. J. Mol. Liq. 2019; **285**(1):96–105.

[79] Suh J, Lee E, Myoung YC, Kim M, Kim S. Effect of the cinnomyl group on liquid crystal aligning capabilities on PCEMA surface. J. Org. Chem. 2001; **28**(3):333-337.

[80] Halim M, Tremblay MS, Jockusch S, et al. Transposing molecular fluorescent switches into the near-IR: Development of luminogenic reporter substrates for redox metabolism. Journal of the American Chemical Society. 2007; **129**(1):7704–7705.

[81] Gray GW. Molecular Structures and Properties of Liquid Crystals. (Academic Press, London), 288, 1962.